

Secure Communications for All Users in Low-Resolution IRS-aided Systems Under Imperfect and Unknown CSI

Monir Abughalwa *Student Member, IEEE*, Diep N. Nguyen, *Senior Member, IEEE*,
Dinh Thai Hoang, *Senior Member, IEEE*, Thang X. Vu, *Senior Member, IEEE*,
Eryk Dutkiewicz, *Senior Member, IEEE*, and Symeon Chatzinotas, *Fellow, IEEE*

Abstract—Provisioning secrecy for *all users*, given the heterogeneity and uncertainty of their channel conditions, locations, and the unknown location of the attacker/eavesdropper, is challenging and not always feasible. This work takes the first step to guarantee secrecy for all users where a low resolution intelligent reflecting surfaces (IRS) is used to enhance legitimate users' reception and thwart the potential eavesdropper (Eve) from intercepting. In real-life scenarios, due to hardware limitations of the IRS' passive reflective elements (PREs), the use of a full-resolution (continuous) phase shift (CPS) is impractical. In this paper, we thus consider a more practical case where the phase shift (PS) is modeled by a low-resolution (quantized) phase shift (QPS) while addressing the phase shift error (PSE) induced by the imperfect channel state information (CSI). To that end, we aim to maximize the minimum secrecy rate (SR) among *all users* by jointly optimizing the transmitter's beamforming vector and the IRS's passive reflective elements (PREs) under perfect/imperfect/unknown CSI. The resulting optimization problem is non-convex and even more complicated under imperfect/unknown CSI. To tackle it, we linearize the objective function, and decompose the problem into sequential subproblems. When the perfect CSI is not available, we use the successive convex approximation (SCA) approach to transform imperfect CSI related semi-infinite constraints into finite linear matrix inequalities (LMI). We prove that our proposed algorithm converges to a locally optimal solution with low computational complexity thanks to our closed-form linearization approach. This makes the solution scalable for large IRS deployments. Extensive simulations with practical settings show that our approach can ensure secure communication for all users while the IRS's PREs are quantized and are affected by the PSE.

Index Terms—Low resolution/quantized phase shift (QPS), phase shift error (PSE), intelligent reflective surfaces (IRS), artificial noise (AN), continuous phase shift (CPS), and secrecy rate (SR) fairness.

I. INTRODUCTION

Intelligent reflective surface (IRS) is a promising technology that has attracted paramount interest. IRSs comprise passive reflective elements (PRE) with a phase shift (PS) controller to tailor the reflected signals upon them [1]. By optimizing signal reflections, IRSs improve reception by creating favorably reflected multi-path signals at receivers. Thanks to their cost-effective design and convenient deployment typically on the facades of high-rise buildings, IRSs hold immense potential for various applications, particularly in urban areas

Monir Abughalwa, Diep N. Nguyen, Dinh Thai Hoang, and Eryk Dutkiewicz are with School of Electrical and Data Engineering, University of Technology Sydney, Sydney, Australia (e-mail: monir.abughalwa@student.uts.edu.au; diep.nguyen@uts.edu.au; hoang.dinh@uts.edu.au; eryk.dutkiewicz@uts.edu.au).

Thang X. Vu, and Symeon Chatzinotas are with the Interdisciplinary Centre for Security Reliability and Trust (SnT), Universite du Luxembourg, Luxembourg, Luxembourg (e-mail: thang.vu@uni.lu; symeon.chatzinotas@uni.lu).

Preliminary results of this work are presented at the IEEE GLOBECOM Conference, 2024, [?].

where line-of-sight channels between transmitters (Tx) and receivers (Rx) frequently face obstructions [2]. Particularly, for the Internet of Things (IoT) devices that are limited computing capability and battery/energy, the IRS has gained paramount attention aiming to enhance both spectral and energy efficiency [3].

A. Related Works and Motivations

Another potential application of IRSs is to enhance the security/privacy of users by purposely manipulating reflected signals from the Tx so as to facilitate the signal reception at legitimate users while maximizing the multi-user interference/degrading the signals at potential eavesdroppers. In [4], the authors studied the design of an IRS to maximize the legitimate user's secrecy rate (SR), which is defined as the difference between the rate of the legitimate channel and that of the channel from the transmitter to a potential eavesdropper. The authors studied SR maximization by jointly optimizing the beamforming vector at the transmitter and the IRS' PREs. A multi-input-single-output (MISO) IRS-aided system with the presence of multiple eavesdroppers was considered in [5]. The transmitter introduced artificial noise (AN) as a countermeasure to enhance user security. In [6], the authors studied a cell-free IRS-aided network, where they aimed to enhance the user's secrecy by maximizing the weighted sum of the users' secrecy rate (WSSR) by jointly optimizing the beamforming vector and the IRS's PREs. AO algorithm was used to decouple the beamforming factor and the IRS' PREs, and the resulting problem was tackled using the semi-definite relaxation (SDR) and continuous convex approximation. Shi et al. in [7] investigated the SR in a multi-input multi-output (MIMO) IRS-aided system with the presence of a single eavesdropper. The IRS was deployed to enhance the uplink transmission and the downlink energy transfer. The authors investigated the problem of SR maximization by jointly optimizing the transmit beamform vector, the downlink/uplink time allocation, and the energy transmit covariance matrix.

When the channel state information (CSI) from the IRS to the users/receivers is unknown or imperfect, the authors in [8] studied an IRS-aided multi-user system, where they formulated a secrecy sum rate (SSR) maximization problem with the eavesdropper's channel partially known to the receiver. In [9], the authors investigated an IRS-aided cognitive radio system when the eavesdropper's CSI is not available at Alice. The authors proposed a power minimization problem to guarantee users' secrecy by optimizing the beamforming vector and the IRS PREs which were modeled by continuous PS. It is worth mentioning that most of the research in IRS's secrecy and signal-to-interference plus noise ratio (SINR) maximization, assumes perfect phase estimation and/or full resolution/continuous phase shift (CPS) [4], [6], [10].

However, assuming CPS of the IRS's PREs is not practical in real-life scenarios due to hardware limitation [11]. In [12] the authors studied an IRS-aided system with a discrete/quantized phase shift (QPS). The authors proposed a transmission power minimization problem to achieve a certain user's SNR by jointly optimizing the beamforming vector and the discrete PREs. In [13], it was shown that using a 3-bit QPS can nearly achieve the same performance as a CPS. When the transmitter can obtain partial/imperfect CSI, the IRS' PREs are affected by phase shift error (PSE). The PSE was investigated in [14], where the IRS PREs PSE was presented in in large IRS system.

Motivated by the above, this paper aims to achieve secrecy for *all users* under low resolution IRS-aided systems with both perfect and imperfect CSI. To that end, we consider a popular use case where a low resolution IRSs is used to enhance/aid the signal reception at legitimate users (from a transmitter) in the presence of a potential eavesdropper. We then maximize the minimum SR by optimizing the transmit beamforming vector and the IRS's PREs.

When only partial or erroneous CSI (from the IRS to the users and the eavesdropper) is available, the problem is even more challenging due to the semi-infinite constraints invoked by the imperfect CSI and the IRS's PREs PSE. To tackle the problem, we first introduce slack variables to deal with the transmitter's beamforming vectors and the IRS's PREs coupling within the objective function. Secondly, we leverage the successive convex approximation (SCA) technique [15], and the S -procedure [16] to convert the semi-infinite constraints into linear matrix inequalities (LMI). Then, we propose a penalty convex-concave procedure (PCCP) [17] to tackle the unit modulus constraint (UMC) of IRSs. It is worth mentioning that, unlike existing approaches, e.g., [18] that usually assume the eavesdropper can somehow remove all interference to deal with imperfect CSI, here we tackle a more realistic scenario where the eavesdropper is affected by the multi-user interference. For comparison purposes, we also consider the SSR maximization problem. When the eavesdropper's CSI is unknown to the transmitter, the IRS PREs modeled by QPS suffer from PSE. To provide secrecy for all users, we develop a power minimization problem while introducing a residual power that acts as AN to lower the eavesdropper's SINR. Extensive simulations with practical settings show that by maximizing the minimum SR among all the users or minimizing transmit power and using AN, we can achieve a better chance of ensuring secure communications for *all users* (subject to the location of the eavesdropper) even under imperfect CSI and low-resolution IRS. Where feasible, as expected, we observe that maximizing the minimum SR can achieve greater fairness among the users compared to the SSR maximization problem.

B. Contributions

The main contributions are summarized as follows:

- First, we study the SR guarantee for *all users* and the impact of the low resolution IRS in a multi-user downlink IRS-aided network. We formulate three optimization problems: maximizing the minimum SR, maximizing the SSR, and minimizing the transmission power, by jointly optimizing the transmitter's beamforming vector and the IRS's PREs. We then study the problems under both perfect and imperfect CSI cases.
- When the CSI is available, we tackle the above non-convex problem by linearizing its objective function with tractable approximation functions, leading to a computationally efficient algorithm. To tackle UMC, unlike traditional methods, i.e. conventional SDR, we directly

optimize the quantized PREs arguments to provide a low-complexity solution that can scale with large IRSs. The resulting solution is proved to converge to a locally optimal solution of the original non-convex problem.

- When perfect CSI is not available, we use the successive convex approximation (SCA) approach to transform imperfect CSI related semi-infinite constraints into finite linear matrix inequalities (LMI). We prove that our proposed algorithm's converges to a locally optimal solution with low computational complexity thanks to our closed-form linearization approach. This makes the solution scalable for large IRS deployments.
- Eventually, we perform extensive simulations to evaluate the impact of optimizing the IRS's PREs on the users' SR. We observe that the proposed algorithms can guarantee secure communication for all users, On the other hand, the approaches that focus on maximizing the SSR, i.e. [19], do not guarantee secrecy to all users.

The remainder of this paper is organized as follows. The system model is discussed in Sections II. Then, Sections III, IV and V present the problem and corresponding solutions under perfect/imperfect/unknown CSI, respectively. The extensive simulations and discussion are in Section VI. Finally, Section VII concludes the paper and discusses potential future directions.

This paper uses the following notation: bold letters denote vectors and matrices. \mathbf{I}_M denotes an M dimensional identity matrix. $\text{Diag}(n_1, \dots, n_n)$ denotes the diagonal matrix with diagonal entries of $\{n_1, \dots, n_n\}$. The symbols \Re and \mathbb{C} represent the real and the complex field, respectively. $\mathcal{C}(0, \bar{z})$ denotes the circular Gaussian random variable with zero mean and variance \bar{z} . For matrices \mathbf{C} and \mathbf{D} , $\langle \mathbf{C}, \mathbf{D} \rangle \triangleq \text{trace}(\mathbf{C}^H \mathbf{D})$. For matrix \mathbf{A} , $\Re\{\mathbf{A}\}$ denotes the real part, $\langle \mathbf{A} \rangle \triangleq \text{trace}(\mathbf{A})$, the symbol $\|\mathbf{A}\|_1$ denotes the 1-norm, $\|\mathbf{A}\|$ denotes the Frobenius norm, \mathbf{A}^* denotes the conjugate, \mathbf{A}^H denotes the Hermitian (conjugate transpose), $\lambda_{\max}(\mathbf{A})$ denotes the maximal eigenvalue, $\angle(\mathbf{A})$ denotes its argument, and $\mathbf{A} \succeq 0$ means positive semi-definite.

II. SYSTEM MODEL

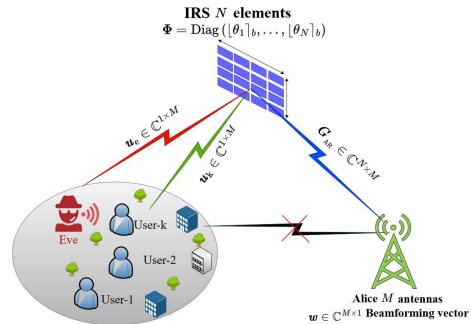


Fig. 1: System Model.

We consider a low resolution IRS-aided downlink system as depicted in Fig. 1, in which an M -antenna transmitter (Alice) transmits confidential information to \mathcal{K} single antenna users under the presence of a single antenna eavesdropper (Eve) that attempts to wiretap the transmission. An IRS with (N) PREs is deployed (e.g., at the facade of a building) to support the transmission between Alice and the users. Let

$k \triangleq \{1, 2, \dots, K\}$ denote the set of the legitimate users and e denote the Eve in the system. Let $\mathbf{h}_{A_i} \triangleq \sqrt{\beta_{A_i}} \tilde{\mathbf{h}}_{A_i}$ denote the direct channel from Alice to the users/Eve modeled by Rician fading, $\tilde{\mathbf{h}}_{A_i}$ is modelled by Rician fading, and $\sqrt{\beta_{A_i}}$ is the large scale fading from the Alice-to-users/Eve link, $\mathbf{G}_{AR} \triangleq \sqrt{\beta_{AR}} \tilde{\mathbf{G}}_{AR} \in \mathbb{C}^{N \times M}$ denote the channel from Alice to the IRS, while $\tilde{\mathbf{G}}_{AR}$ is modeled by Rician fading, and $\sqrt{\beta_{AR}}$ is the large scale fading factor of the Alice-to-IRS link. The channel from the IRS to user k and to Eve is modeled by $\mathbf{u}_i \triangleq \sqrt{\beta_{Ri}} \tilde{\mathbf{u}}_i \mathbf{R}_{Ri}^{1/2} \in \mathbb{C}^{1 \times N}$, where $i \in \{k, e\}$, β_{Ri} is the large-scale fading factor of the IRS-to- i [20], $\tilde{\mathbf{u}}_i$ is modeled by Rician fading, and $\mathbf{R}_{Ri} \in \mathbb{C}^{N \times N}$ is the IRS elements' spatial correlation matrix [20]. For the confidential message intended for user k , s_k , the signal received by user k and Eve with corresponding to the intended user can be respectively expressed by:

$$y_i \triangleq \mathbf{h}_i(\boldsymbol{\theta}) \sum_{k=1}^{\mathcal{K}} \mathbf{w}_k s_k + n_i, \quad i \in \{k, e\}, \quad (1)$$

where $\mathbf{h}_i(\boldsymbol{\theta}) \in \mathbb{C}^{1 \times M}$ is the cascaded channel gain from Alice to $i \in \{k, e\}$, $\mathbf{w}_k \in \mathbb{C}^{M \times 1}$ is the beamforming vector applied for user k , $\boldsymbol{\theta} \triangleq (\theta_1, \dots, \theta_N)^T \in [0, 2\pi)^N$ denotes the IRS's PREs PS vector, n_i is the zero-mean Additive White Gaussian Noise (AWGN) with power σ_i for $i \in \{k, e\}$. The cascade channel gain $\mathbf{h}_i(\boldsymbol{\theta})$ from Alice to $i \in \{k, e\}$, can be written in terms of the channel gain from Alice to the users/Eve, Alice to the IRS and the channel gain from the IRS to the user or Eve as follows:

$$\mathbf{h}_i(\boldsymbol{\theta}) \triangleq \mathbf{u}_i \boldsymbol{\Phi} \mathbf{G}_{AR} \triangleq \mathbf{u}_i \sum_{n=1}^N \exp(j\theta_n) \Xi_n \mathbf{G}_{AR}, \quad (2)$$

where $\boldsymbol{\Phi} \triangleq \text{Diag}(e^{j\theta})$, Ξ_n is an $N \times N$ matrix with all zeros except for its (n, n) entry which is 1.

The CSI from Alice to the IRS/users can be estimated by calculating the angle of arrival and departure [19]. However, the reflected channel's CSI from the IRS to the IoT users is much more challenging to obtain due to the passive nature of the IRS and the mobility/varying nature of the users' environment and location [21]. For Eve, it is also hardly possible to pinpoint its location or its accurate CSI from the IRS. To account for the CSI imperfection, we adopt the bounded CSI model in which the reflected channel from the IRS to the users and Eve can be expressed as [22]:

$$\mathbf{u}_i \triangleq \hat{\mathbf{u}}_i + \Delta \mathbf{u}_i, \quad i \in \{k, e\}, \quad (3a)$$

$$\omega_i \triangleq \{\|\Delta \mathbf{u}_i\|_2 \leq \xi_i\}, \quad i \in \{k, e\}, \quad (3b)$$

where $\hat{\mathbf{u}}_i$ denotes the (imperfect) estimated channel vector, $\Delta \mathbf{u}_i$ represents the channel estimation error of the corresponding estimation, ω_i is a set for all possible channel estimation errors, and ξ_i is the radii of the uncertainty regions as known to Alice. Hence, (2) can be reformulated as:

$$\hat{\mathbf{h}}_i(\boldsymbol{\theta}) \triangleq (\hat{\mathbf{u}}_i + \Delta \mathbf{u}_i) \boldsymbol{\Phi} \mathbf{G}_{AR}. \quad (4)$$

Hence, we can write the corresponding signal-to-interference-plus-noise ratio (SINR) of the received signal of the user- k and Eve under perfect/imperfect CSI as:

$$\gamma_i(\mathbf{w}, \boldsymbol{\theta}) \triangleq \frac{|\mathbf{h}_i(\boldsymbol{\theta}) \mathbf{w}_k|^2}{\rho_i(\mathbf{w}, \boldsymbol{\theta})}, \quad i \in \{k, e\}, \quad (5)$$

$$\hat{\gamma}_i(\mathbf{w}, \boldsymbol{\theta}) \triangleq \frac{|\hat{\mathbf{h}}_i(\boldsymbol{\theta}) \mathbf{w}_k|^2}{\hat{\rho}_i(\mathbf{w}, \boldsymbol{\theta})}, \quad i \in \{k, e\}, \quad (6)$$

where $\rho_i(\mathbf{w}, \boldsymbol{\theta}) \triangleq \sum_{j=1, j \neq k}^{\mathcal{K}} |\mathbf{h}_i(\boldsymbol{\theta}) \mathbf{w}_j|^2 + \sigma_i$, and $\hat{\rho}_i(\mathbf{w}, \boldsymbol{\theta}) \triangleq \sum_{j=1, j \neq k}^{\mathcal{K}} |\hat{\mathbf{h}}_i(\boldsymbol{\theta}) \mathbf{w}_j|^2 + \sigma_i$. However, in a low-resolution IRS-aided system with imperfect CSI from the IRS to the

users/Eve, the IRS PREs are affected by PSE [14]. Thus, in the following, we consider three cases to model the IRS' PREs as:

- The CPS adjustment at the IRS; this is the ideal case when the IRS PREs can be modeled by a continuous PS.
- The low resolution/QPS at the IRS; where the PS can be modeled by a uniform distribution in $[\boldsymbol{\theta}]_b \in [\frac{-\pi}{2^b}, \frac{\pi}{2^b})$, where b is the number of bits in the QPS modulation.
- with imperfect/unknown CSI, and when only a discrete set of 2^b phases can be configured; this leads to a PSE ϵ_R which can be approximated by a uniform distribution in $[-2^{-b}\pi, 2^{-b}\pi)$, hence, (1) can be reformulated as:

$$\mathbf{h}_i([\boldsymbol{\theta}]_b) \triangleq \mathbf{u}_i \text{Diag}(e^{j([\boldsymbol{\theta}]_b + \epsilon_R)}) \mathbf{G}_{AR}. \quad (7)$$

In the sequel, we deal with both perfect and imperfect CSI from the IRS to the users and Eve. In the latter, only partial/imperfect CSI $\hat{\mathbf{u}}_i$ is available. In this case, one can vary the magnitude of $\Delta \mathbf{u}_i$, i.e., the radii ξ_i of the uncertainty region to capture different levels of CSI imperfection. In a more extreme case, we assume only partial/imperfect IRS-to-users' CSI can be obtained by Alice, and Eve's CSI is unknown to Alice.

Under the presence of Eve, the closed-form expression for the SR of the user- k under perfect/imperfect/unknown IRS to users/Eve CSI is defined as [23]:

$$\text{SR}_k(\mathbf{w}, [\boldsymbol{\theta}]_b) \triangleq [C_k(\mathbf{w}, \boldsymbol{\theta}) - C_e(\mathbf{w}, \boldsymbol{\theta})]^+, \quad (8)$$

$$\widehat{\text{SR}}_k(\mathbf{w}, [\boldsymbol{\theta}]_b) \triangleq [\widehat{C}_k(\mathbf{w}, \boldsymbol{\theta}) - \widehat{C}_e(\mathbf{w}, \boldsymbol{\theta})]^+, \quad (9)$$

Where $[x]^+ \triangleq \max[0, x]$, the user- k data rate, and the eavesdropping rate under perfect/imperfect CSI are defined as [23]:

$$C_i(\mathbf{w}, [\boldsymbol{\theta}]_b) \triangleq \ln(1 + \gamma_i(\mathbf{w}, \boldsymbol{\theta})), \quad i \in \{k, e\}, \quad (10)$$

$$\widehat{C}_i(\mathbf{w}, [\boldsymbol{\theta}]_b) \triangleq \ln(1 + \hat{\gamma}_i(\mathbf{w}, \boldsymbol{\theta})), \quad i \in \{k, e\}. \quad (11)$$

III. MINIMUM USER'S SR MAXIMIZATION UNDER PERFECT CSI

A. MAXMIN SR under perfect CSI

In this section, we first address the problem of maximizing the minimum SR among all the users, under perfect CSI assumption, to guarantee secure communications for all users. The optimization problem can be formally stated as

$$(P1) : \max_{\mathbf{w}, [\boldsymbol{\theta}]_b} \min_{k \in \mathcal{K}} \text{SR}_k(\mathbf{w}, [\boldsymbol{\theta}]_b), \quad (12a)$$

$$\text{s.t.} \quad \sum_{k=1}^{\mathcal{K}} \|\mathbf{w}_k\|^2 \leq P_T, \quad (12b)$$

$$|e^{(j[\boldsymbol{\theta}]_b)}| = 1, \quad (12c)$$

where P_T is the transmit power, (12b) captures the sum of the transmitted power constraint, and (12c), captures the UMC of the PREs' PS.

The optimization problem (P1) is nonconvex since the objective function (12a) is not concave and the UMC (12c) is nonconvex. To tackle this nonconvex problem, one can employ the AO technique [1]. Specifically, at iteration (ι) , the feasible point $(\mathbf{w}^{(\iota)}, [\boldsymbol{\theta}^{(\iota)}]_b)$ is generated from (P1) by solving two sub-problems, the first one is to optimize \mathbf{w} with a fixed $[\boldsymbol{\theta}]_b$,

$$(P1.1) : \max_{\mathbf{w}} \min_k \text{SR}_k(\mathbf{w}, [\boldsymbol{\theta}^{(\iota)}]_b), \quad \text{s.t.} (12b),$$

then, we optimize $[\boldsymbol{\theta}]_b$ with a fixed \mathbf{w} by solving the following AO problem,

$$(P1.2) : \max_{[\boldsymbol{\theta}]_b} \min_k \text{SR}_k(\mathbf{w}^{(\iota+1)}, [\boldsymbol{\theta}]_b), \quad \text{s.t.} (12c).$$

$$C_e(\mathbf{w}, [\boldsymbol{\theta}^{(\iota)}]_b) \geq q_{1,k_e}^{(\iota)} + 2\Re \sum_{j=1, j \neq k}^K \left\{ \langle \mathbf{m}_{j,k_e}^{(\iota)}, \mathbf{w}_j \rangle \right\} - \frac{\rho_e^{(\iota)}}{1 + \rho_e^{(\iota)}} \left(\sum_{j=1, j \neq k}^K |\mathbf{h}_e([\boldsymbol{\theta}^{(\iota)}]_b) \mathbf{w}_j|^2 \right) - \frac{1}{v_e^{(\iota)}} \sum_{j=1}^K |\mathbf{h}_e([\boldsymbol{\theta}^{(\iota)}]_b) \mathbf{w}_j|^2. \quad (15)$$

$$\boldsymbol{\psi}_k^{(\iota)} \triangleq \sum_{j=1}^K n_{1,k}^{(\iota+1)} \mathbf{h}_k^H([\boldsymbol{\theta}^{(\iota)}]_b) \mathbf{h}_k([\boldsymbol{\theta}^{(\iota)}]_b) + \frac{\rho_e^{(\iota)}}{1 + \rho_e^{(\iota)}} \sum_{j=1, j \neq k}^K \mathbf{h}_e^H([\boldsymbol{\theta}^{(\iota)}]_b) \mathbf{h}_e([\boldsymbol{\theta}^{(\iota)}]_b) + \frac{1}{v_e^{(\iota)}} \sum_{j=1}^K \mathbf{h}_e^H([\boldsymbol{\theta}^{(\iota)}]_b) \mathbf{h}_e([\boldsymbol{\theta}^{(\iota)}]_b), \quad (17)$$

$$C_k(\mathbf{w}^{(\iota+1)}, [\boldsymbol{\theta}]_b) \geq q_{1,k}^{(\iota+1)} + 2\Re \left\{ \sum_{n=1}^N \mathbf{m}_{k,k}^{(\iota+1)}(n) e^{j[\boldsymbol{\theta}_n]_b} \right\} + \left(e^{j[\boldsymbol{\theta}]_b} \right)^H \boldsymbol{\varphi}_{1,k}^{(\iota+1)} e^{j[\boldsymbol{\theta}]_b}, \quad (19)$$

$$q_{1,k}^{(\iota+1)} \triangleq C_k(\mathbf{w}^{(\iota+1)}, [\boldsymbol{\theta}^{(\iota)}]_b) - \gamma_k(\mathbf{w}^{(\iota+1)}, [\boldsymbol{\theta}^{(\iota)}]_b) - \sigma_k n_{1,k}^{(\iota+1)}, \quad (20)$$

$$n_{1,k}^{(\iota+1)} \triangleq 1/\rho_k^{(\iota+1)} - 1/v_k^{(\iota+1)}, \quad (21)$$

However, with AO, solving two subproblems (P1.1) and (P1.2) is computationally demanding, especially given the large number of PREs of the IRS. Our proposed linearization method in the sequel uses mathematically tractable approximation functions leading to a computationally efficient algorithm that can be used for a large number of IRS's PREs.

1) *Sub-Problem for Optimizing the Beamforming Vectors:* We fix $[\boldsymbol{\theta}]_b$ given $\mathbf{w}^{(\iota)}$ and solve the problem (P1.1) to obtain $\mathbf{w}^{(\iota+1)}$ satisfying $\text{SR}_k(\mathbf{w}^{(\iota+1)}, [\boldsymbol{\theta}^{(\iota)}]_b) > \text{SR}_k(\mathbf{w}^{(\iota)}, [\boldsymbol{\theta}^{(\iota)}]_b)$. We start by linearizing the objective function in (12a), which consists of two parts, User- k 's data rate and Eve's negative eavesdropping rate. First, we transfer the user- k 's data rate into a linear form. Specifically, using the inequality (65) in Appendix D, let's define $\boldsymbol{\Lambda} \triangleq \mathbf{h}_k([\boldsymbol{\theta}]_b) \mathbf{w}_k$, $\mathbf{F} \triangleq \rho_k(\mathbf{w}, [\boldsymbol{\theta}^{(\iota)}]_b)$, $\hat{\boldsymbol{\Lambda}} \triangleq \mathbf{h}_k([\boldsymbol{\theta}^{(\iota)}]_b) \mathbf{w}_k^{(\iota)}$ and $\hat{\mathbf{F}} \triangleq \rho_k(\mathbf{w}^{(\iota)}, [\boldsymbol{\theta}^{(\iota)}]_b)$, hence, the users' data rate (10) can be written as

$$C_k(\mathbf{w}, [\boldsymbol{\theta}^{(\iota)}]_b) \geq q_{1,k}^{(\iota)} + 2\Re \left\{ \langle \mathbf{m}_{k,k}^{(\iota)}, \mathbf{w}_k \rangle \right\} - n_{1,k}^{(\iota)} v_k^{(\iota)}, \quad (13)$$

where,

$$\begin{aligned} v_k^{(\iota)} &\triangleq \sum_{j=1}^K |\mathbf{h}_k([\boldsymbol{\theta}^{(\iota)}]_b) \mathbf{w}_j|^2 + \sigma_k, \\ q_{1,k}^{(\iota)} &\triangleq C_k(\mathbf{w}, [\boldsymbol{\theta}^{(\iota)}]_b) - \gamma_k(\mathbf{w}, [\boldsymbol{\theta}^{(\iota)}]_b) - \sigma_k n_{1,k}^{(\iota)}, \\ \mathbf{m}_{k,k}^{(\iota)} &\triangleq (\mathbf{h}_k^H([\boldsymbol{\theta}^{(\iota)}]_b) \mathbf{h}_k([\boldsymbol{\theta}^{(\iota)}]_b) \mathbf{w}_k) / (\rho_k^{(\iota)}), \\ n_{1,k}^{(\iota)} &\triangleq 1/\rho_k^{(\iota)} - 1/v_k^{(\iota)}. \end{aligned}$$

Second, we linearize Eve's negative eavesdropping rate, which can be expressed as:

$$-\ln(1 + \gamma_e(\mathbf{w}, [\boldsymbol{\theta}^{(\iota)}]_b)) \triangleq \overbrace{\ln(1 + \rho_e^{(\iota)})}^{a_1} - \overbrace{\ln(1 + v_e^{(\iota)})}^{a_2}, \quad (14)$$

where $v_e^{(\iota)} \triangleq \sum_{j=1}^K |\mathbf{h}_e([\boldsymbol{\theta}^{(\iota)}]_b) \mathbf{w}_j|^2 + \sigma_e$. Here we adopt the idea in [24], where the term (a_1) in (14) can be linearized by defining $\mathbf{z} \triangleq \rho_e^{(\iota)}$ and substituting it in the inequality (66) in Appendix D. The term (a_2) in (14) can be linearized by defining $\boldsymbol{\Upsilon} \triangleq v_e^{(\iota)}$ and substituting it in the inequality (72) in Appendix D.

Hence, Eve's eavesdropper rate can be expressed as in (15), where,

$$\begin{aligned} q_{1,k_e}^{(\iota)} &\triangleq \ln(\rho_e^{(\iota)}) - \rho_e^{(\iota)} - \ln(v_e^{(\iota)}) + n_{1,k_e}^{(\iota)} + 1, \\ n_{1,k_e}^{(\iota)} &\triangleq \left(-\frac{\rho_e^{(\iota)}}{1 + \rho_e^{(\iota)}} - \frac{1}{v_e^{(\iota)}} \right) \sigma_e, \\ \mathbf{m}_{j,k_e}^{(\iota)} &\triangleq \mathbf{h}_e^H([\boldsymbol{\theta}^{(\iota)}]_b) \mathbf{h}_e([\boldsymbol{\theta}^{(\iota)}]_b) \mathbf{w}_j. \end{aligned}$$

By substituting (13) and (15) into (8), we can express the closed-form SR as

$$\text{SR}_k(\mathbf{w}, [\boldsymbol{\theta}^{(\iota)}]_b) \geq q_k^{(\iota)} + 2\Re \left\{ \langle \mathbf{m}_k^{(\iota)}, \mathbf{w}_k \rangle \right\} - (\mathbf{w}_k)^H \boldsymbol{\psi}_k^{(\iota)} \mathbf{w}_k, \quad (16)$$

where $\boldsymbol{\psi}_k^{(\iota)}$ is defined in (17), and

$$\begin{aligned} q_k^{(\iota)} &\triangleq q_{1,k}^{(\iota)} + q_{1,k_e}^{(\iota)} + n_{1,k_e}^{(\iota)}, \\ \mathbf{m}_k^{(\iota)} &\triangleq \mathbf{m}_{k,k}^{(\iota)} + \sum_{j=1, j \neq k}^K \tilde{\mathbf{m}}_{j,k}^{(\iota)}, \\ \tilde{\mathbf{m}}_{j,k}^{(\iota)} &\triangleq \mathbf{h}_e^H([\boldsymbol{\theta}^{(\iota)}]_b) \mathbf{h}_e([\boldsymbol{\theta}^{(\iota)}]_b) \mathbf{w}_j. \end{aligned}$$

Finally, with (16), problem (P1.1) can be reformulated as the following problem (P1.2)

$$(\mathcal{P}1.3) : \max_{\Gamma, \mathbf{w}}, \quad (18a)$$

$$\text{s.t.} \quad \Gamma \leq \text{SR}_k(\mathbf{w}, [\boldsymbol{\theta}^{(\iota)}]_b), \quad \forall k, \quad (18b)$$

$$(12b), \quad (18c)$$

where Γ is an auxiliary variable as the lower bound of the SR. Problem (P1.3) is an SDP problem with its linearized objective function in (16). This problem can be solved using standard solvers, e.g., the interior point method or the CVX toolbox [25].

2) *Sub-Problem for Optimizing the PREs:* Similarly, by fixing \mathbf{w} , we aim to find $[\boldsymbol{\theta}^{(\iota+1)}]_b$ such that, $\text{SR}_k(\mathbf{w}_k^{(\iota+1)}, [\boldsymbol{\theta}^{(\iota+1)}]_b) > \text{SR}_k(\mathbf{w}_k^{(\iota+1)}, [\boldsymbol{\theta}^{(\iota)}]_b)$. Following the same method in the previous section, the lower bound approximation of the user's data rate can be obtained by using the inequality (65) in Appendix D. The user's data rate can be expressed as in (19), where $q_{1,k}^{(\iota+1)}$ is given in (20), $n_{1,k}^{(\iota+1)}$ is given in (21), and,

$$\begin{aligned} \mathbf{m}_{k,k}^{(\iota+1)}(n) &\triangleq \hat{\mathbf{m}}_{k,k}^{(\iota+1)}(n) / \rho_k^{(\iota+1)}, \\ \hat{\mathbf{m}}_{k,k}^{(\iota+1)}(n) &\triangleq \left(\mathbf{w}_k^{(\iota+1)} \right)^H \mathbf{h}_k^H([\boldsymbol{\theta}^{(\iota)}]_b) \mathbf{u}_k \Xi_n \mathbf{G}_{\text{AR}} \mathbf{w}_k^{(\iota+1)}, \\ \boldsymbol{\varphi}_{1,k}^{(\iota+1)} &\triangleq -n_{1,k}^{(\iota+1)} \sum_{j=1}^K \boldsymbol{\varphi}_{k,j}^{(\iota+1)}, \\ \boldsymbol{\varphi}_{k,j}^{(\iota+1)} &\triangleq \left(\mathbf{N}_{k,j}^{(\iota+1)}(n) \right)^* \mathbf{N}_{k,j}^{(\iota+1)}(m), \quad n \in N, m \in N, \\ \mathbf{N}_{k,j}^{(\iota+1)}(n) &\triangleq \mathbf{u}_k \Xi_n \mathbf{G}_{\text{AR}} \mathbf{w}_j^{(\iota+1)}. \end{aligned}$$

Similarly, we can express Eve's eavesdropping rate as in (22),

$$C_e(\mathbf{w}^{(\iota+1)}, \lfloor \boldsymbol{\theta} \rfloor_b) \geq q_{1,k_e}^{(\iota+1)} + 2\Re \left\{ \sum_{n=1}^N \mathbf{m}_{k_e}^{(\iota+1)}(n) e^{j\lfloor \theta_n \rfloor_b} \right\} + \left(e^{j\boldsymbol{\theta}} \right)^H \boldsymbol{\varphi}_{1,k_e}^{(\iota+1)} e^{j\lfloor \boldsymbol{\theta} \rfloor_b} + \left(e^{j\lfloor \boldsymbol{\theta} \rfloor_b} \right)^H \boldsymbol{\varphi}_{k_e,j}^{(\iota+1)} e^{j\lfloor \boldsymbol{\theta} \rfloor_b}, \quad (22)$$

$$q_k^{(\iota+1)} \triangleq q_{1,k}^{(\iota+1)} + q_{1,k_e}^{(\iota+1)} - \left(e^{j\lfloor \boldsymbol{\theta}^{(\iota)} \rfloor_b} \right)^H \tilde{\boldsymbol{\varphi}}_k^{(\iota+1)} e^{j\lfloor \boldsymbol{\theta}^{(\iota)} \rfloor_b} - 2\lambda_{\max} \left(\tilde{\boldsymbol{\varphi}}_k^{(\iota+1)} \right) N, \quad (24)$$

$$\mathbf{m}_k^{(\iota+1)}(n) \triangleq \hat{\mathbf{m}}_{k,k}^{(\iota+1)}(n) + \tilde{\mathbf{m}}_k^{(\iota+1)}(n) + \sum_{m=1}^N e^{-j\lfloor \theta_m^{(\iota)} \rfloor_b} \tilde{\boldsymbol{\varphi}}_k^{(\iota+1)}(m, n) + \lambda_{\max} \left(\tilde{\boldsymbol{\varphi}}_k^{(\iota+1)} \right), \quad (25)$$

$$\lfloor \boldsymbol{\theta}^{(\iota+1)} \rfloor_b \triangleq \arg \max_{\lfloor \boldsymbol{\theta} \rfloor_b \in \{ \lfloor \boldsymbol{\theta} \rfloor_b^{(\iota+1),k}, k=1, \dots, K \}} \text{SR}_k(\mathbf{w}^{(\iota+1)}, \lfloor \boldsymbol{\theta} \rfloor_b). \quad (28)$$

Algorithm 1 Proposed Iterative Algorithm for Solving Problem (P1)

- 1: **Initialize:** $(\mathbf{w}^{(1)}, \lfloor \boldsymbol{\theta} \rfloor_b^{(1)})$, convergence tolerance $\epsilon_t > 0$, and Set $\iota = 1$.
- 2: **Repeat**
- 3: Update $\mathbf{w}^{(\iota+1)}$ by (18), and $\boldsymbol{\theta}^{(\iota+1)}$ by (28);
- 4: **if** $\frac{|\min_k \text{SR}_k(\mathbf{w}^{(\iota+1)}, \lfloor \boldsymbol{\theta}^{(\iota+1)} \rfloor_b) - \min_k \text{SR}_k(\mathbf{w}^{(\iota)}, \lfloor \boldsymbol{\theta}^{(\iota)} \rfloor_b)|}{\min_k \text{SR}_k(\mathbf{w}^{(\iota)}, \lfloor \boldsymbol{\theta}^{(\iota)} \rfloor_b)} \leq \epsilon_t$.
- 5: **Then** $\lfloor \boldsymbol{\theta}^{(\iota)} \rfloor_b \leftarrow \boldsymbol{\theta}^{(\iota+1)}$, $\mathbf{w}^{(\iota)} \leftarrow \mathbf{w}^{(\iota+1)}$ and terminate.
- 6: **Otherwise** $\iota \leftarrow \iota + 1$ and continue.
- 7: **Output** $(\mathbf{w}_k^{(\iota)}, \boldsymbol{\theta}^{(\iota)})$.

Algorithm 2 Proposed AO Algorithm for Solving Problem (P2)

- 1: **Initialize:** $(\mathbf{w}^{(1)}, \lfloor \boldsymbol{\theta}^{(1)} \rfloor_b)$, convergence tolerance $\epsilon_t > 0$, and Set $\iota = 1$.
- 2: **Repeat**
- 3: Update $\mathbf{w}^{(\iota+1)}$ by (32), and $\lfloor \boldsymbol{\theta} \rfloor_b$ by (35);
- 4: **if** $\frac{|\sum_{k=1}^K \text{SR}_k(\mathbf{w}^{(\iota+1)}, \lfloor \boldsymbol{\theta}^{(\iota+1)} \rfloor_b) - \sum_{k=1}^K \text{SR}_k(\mathbf{w}^{(\iota)}, \boldsymbol{\theta}^{(\iota)})|}{\sum_{k=1}^K \text{SR}_k(\mathbf{w}^{(\iota)}, \lfloor \boldsymbol{\theta}^{(\iota)} \rfloor_b)} \leq \epsilon_t$
- 5: **Then** $\lfloor \boldsymbol{\theta}^{(\iota)} \rfloor_b \leftarrow \lfloor \boldsymbol{\theta} \rfloor_b$, $\mathbf{w}^{(\iota)} \leftarrow \mathbf{w}^{(\iota+1)}$ and terminate.
- 6: **Otherwise** $\iota \leftarrow \iota + 1$ and continue.
- 7: **Output** $(\mathbf{w}_k^{(\iota)}, \lfloor \boldsymbol{\theta}^{(\iota)} \rfloor_b)$.

where,

$$q_{1,k_e}^{(\iota+1)} \triangleq \ln \left(\rho_e^{(\iota+1)} \right) - \rho_e^{(\iota+1)} - \ln \left(v_e^{(\iota+1)} \right) + n_{1,k_e}^{(\iota+1)} + 1,$$

$$n_{1,k_e}^{(\iota+1)} \triangleq \left(-\frac{\rho_e^{(\iota+1)}}{1 + \rho_e^{(\iota+1)}} - \frac{1}{v_e^{(\iota+1)}} \right) \sigma_e,$$

$$\mathbf{m}_{k_e}^{(\iota+1)}(n) \triangleq \sum_{j=1, j \neq k}^K \mathbf{m}_{j,k_e}^{(\iota+1)}(n),$$

$$\mathbf{m}_{j,k_e}^{(\iota+1)}(n) \triangleq \left(\mathbf{w}_k^{(\iota+1)} \right)^H \mathbf{h}_e^H \left(\lfloor \boldsymbol{\theta}^{(\iota)} \rfloor_b \right) \mathbf{u}_e \Xi_n \mathbf{G}_{\text{AR}} \mathbf{w}_k^{(\iota+1)},$$

$$\boldsymbol{\varphi}_{1,k_e}^{(\iota+1)} \triangleq \left(\frac{-\rho_e^{(\iota+1)}}{(1 + \rho_e^{(\iota+1)})} - \frac{1}{(\sigma_e + v_e^{(\iota+1)})} \right) \left(\sum_{j=1}^K \boldsymbol{\varphi}_{k_e,j}^{(\iota+1)} \right),$$

$$\boldsymbol{\varphi}_{k_e,j}^{(\iota+1)} \triangleq \left(\mathbf{N}_{k_e,j}^{(\iota+1)}(n) \right)^* \mathbf{N}_{k_e,j}^{(\iota+1)}(m),$$

$$\mathbf{N}_{k_e,j}^{(\iota+1)}(n) \triangleq \mathbf{u}_e \Xi_n \mathbf{G}_{\text{AR}} \mathbf{w}_j^{(\iota+1)}.$$

By combining (19) and (22) into (8), we can express the closed-form SR as:

$$\text{SR}_k(\mathbf{w}^{(\iota+1)}, \lfloor \boldsymbol{\theta} \rfloor_b) \geq q_k^{(\iota+1)} + 2 \sum_{n=1}^N \Re \left\{ \mathbf{m}_k^{(\iota+1)}(n) e^{j\lfloor \theta_n \rfloor_b} \right\}, \quad (23)$$

where $q_k^{(\iota+1)}$ is expressed in (24), $\mathbf{m}_k^{(\iota+1)}(n)$ is expressed in (25), and

$$\boldsymbol{\varphi}_k^{(\iota+1)} \triangleq \boldsymbol{\varphi}_{1,k}^{(\iota+1)} + \boldsymbol{\varphi}_{1,k_e}^{(\iota+1)} + \boldsymbol{\varphi}_{k_e,j}^{(\iota+1)}.$$

With (23), we formulate the following optimization problem to obtain $\lfloor \boldsymbol{\theta}^{(\iota+1)} \rfloor_b$:

$$(\mathcal{P}1.4) : \max_{\lfloor \boldsymbol{\theta} \rfloor_b} \min_{k \in \mathcal{K}} \text{SR}_k \left(\mathbf{w}^{(\iota+1)}, \lfloor \boldsymbol{\theta}^{(\iota)} \rfloor_b \right), \quad (26a)$$

$$\text{s.t.} \quad (12c), \quad (26b)$$

To tackle problem (P1.4) we define

$$\lfloor \theta_n \rfloor_b^{(\iota+1),k} = 2\pi - \angle \mathbf{m}_k^{(\iota+1)}(n), n = 1, \dots, N, \quad (27)$$

then we find $\lfloor \boldsymbol{\theta}^{(\iota+1)} \rfloor_b$ that maximize the $\text{SR}(\mathbf{w}^{(\iota+1)}, \lfloor \boldsymbol{\theta} \rfloor_b)$ as in (28).

The procedure to solve problem (P1) is described in Algorithm 1, which converges to a locally optimal solution of (P1) as formally stated in the following theorem.

Theorem 1: The obtained solution by Algorithm 1 is a locally optimal solution for problem (P1).

Proof: See Appendix A.

3) *Complexity Analysis:* The developed Algorithm 1 is designed to tackle problem (P1) by decoupling the beamforming vector and the IRS's PREs within the objective function. The resulting problem (P1) is an SDP problem that can be solved by the interior point method [25]. The algorithm's complexity can be estimated by its worst-case runtime and the number of the decision variables [26]. Thus, in Algorithm 1, the computational complexity of obtaining \mathbf{w} given $\lfloor \boldsymbol{\theta} \rfloor_b$ is $\mathcal{O}(M^3)$, and the computational complexity of obtaining $\lfloor \boldsymbol{\theta} \rfloor_b$ given \mathbf{w} is $\mathcal{O}(N^3(N+1))$.

B. SSR maximization under perfect CSI

In this section, we address the problem of maximizing the SSR under perfect CSI assumption to achieve users' secrecy. The SSR maximization problem can be stated as:

$$(\mathcal{P}2) : \max_{\mathbf{w}, \lfloor \boldsymbol{\theta} \rfloor_b} \sum_{k=1}^K \text{SR}_k(\mathbf{w}, \lfloor \boldsymbol{\theta} \rfloor_b) \text{ s.t. (12b) \& (12c)}. \quad (29)$$

Similar to the previous section, we seek \mathbf{w} and $\lfloor \boldsymbol{\theta} \rfloor_b$ that maximize the SSR.

1) *Sub-Problem for Optimizing the Beamforming Vectors:* Using (16), the SSR can be expressed as in (30). Therefore, we can rewrite problem (P2) as:

$$(\mathcal{P}2.1) : \max_{\mathbf{w}} \sum_{k=1}^K \text{SR}_k(\mathbf{w}, \lfloor \boldsymbol{\theta}^{(\iota)} \rfloor_b), \text{ s.t. (12b)}. \quad (31)$$

Problem (P2.1) is a convex problem that can be solved using the Lagrangian multiplier method to generate $\mathbf{w}^{(\iota+1)}$

$$\sum_{k=1}^{\mathcal{K}} \text{SR}_k(\mathbf{w}, [\boldsymbol{\theta}^{(\ell)}]_b) \geq \sum_{k=1}^{\mathcal{K}} q_k^{(\ell)} + 2 \sum_{k=1}^{\mathcal{K}} \Re \left\{ \langle \mathbf{m}_k^{(\ell)}, \mathbf{w}_k \rangle \right\} - \sum_{k=1}^{\mathcal{K}} \mathbf{w}_k^H \boldsymbol{\psi}_k^{(\ell)} \mathbf{w}_k, \quad (30)$$

$$\sum_{k=1}^{\mathcal{K}} \text{SR}_k(\mathbf{w}^{(\ell+1)}, [\boldsymbol{\theta}]_b) \geq q^{(\ell+1)} + 2 \sum_{n=1}^N \Re \left\{ \mathbf{m}^{(\ell+1)}(n) e^{j\theta_n} \right\}. \quad (33)$$

as follows [27]:

$$\mathbf{w}_k^{(\ell+1)} \triangleq \begin{cases} (\boldsymbol{\psi}_k^{(\ell)})^{-1} \mathbf{m}_k^{(\ell)} & \text{if } \sum_{k=1}^{\mathcal{K}} \|(\boldsymbol{\psi}_k^{(\ell)})^{-1} \mathbf{m}_k^{(\ell)}\|^2 \leq P_T, \\ (\boldsymbol{\psi}_k^{(\ell)} + \varpi \mathbf{I}_M)^{-1} \mathbf{m}_k^{(\ell)} & \text{otherwise,} \end{cases} \quad (32)$$

where bisection method is used to find ϖ such that

$$\left\| \frac{\mathbf{m}_k^{(\ell)}}{(\boldsymbol{\psi}_k^{(\ell)} + \varpi \mathbf{I}_M)} \right\|^2 = P_T.$$

2) *Sub-Problem for Optimizing the PREs*: In this part, we aim to find $[\boldsymbol{\theta}^{(\ell+1)}]_b$ such that it maximizes the SSR. Using (23), we can express the SSR as in (33), where,

$$q^{(\ell+1)} \triangleq \sum_{k=1}^{\mathcal{K}} q_k^{(\ell+1)},$$

$$\mathbf{m}^{(\ell+1)}(n) \triangleq \sum_{k=1}^{\mathcal{K}} \mathbf{m}_k^{(\ell+1)}(n).$$

We can recast problem (P2) to generate $([\boldsymbol{\theta}^{(\ell+1)}]_b)$ as:

$$(P2.2) : \max_{\boldsymbol{\theta}} \sum_{k=1}^{\mathcal{K}} \text{SR}_k(\mathbf{w}^{(\ell+1)}, [\boldsymbol{\theta}]_b), \text{ s.t. (12c)}, \quad (34a)$$

and the closed-form solution is obtained by,

$$[\boldsymbol{\theta}^{(\ell+1)}]_b = 2\pi - \angle \mathbf{m}^{(\ell+1)}(n), n = 1, \dots, N. \quad (35)$$

Algorithm 2 demonstrates the steps to solve problem (P2). Algorithm 2 converges to at least a locally optimal solution of (P2) as formally stated in the following theorem.

Theorem 2: The obtained solution by the AO Algorithm 2 is a locally optimal solution for problem P2.

Proof: See Appendix C.

3) *Complexity Analysis*: The complexity analysis of Algorithm 2 is similar to that of Algorithm 1. Hence, the complexity of problem P2.1 and problem P2.2 is about $\mathcal{O}(M^3)$ and $\mathcal{O}(N^3(N+1))$, respectively.

IV. DEALING WITH IMPERFECT CSI

A. MAXMIN SR under imperfect CSI

To deal with the imperfect CSI from the IRS to the users and Eve, we adopt the channel modeling in equation (3) where only partial/imperfect channel $\hat{\mathbf{u}}_i$ is available. Nevertheless, In the following analysis, we opt for the case of QPS with PSE, which is the most practical case. One can notice that by setting $b = \infty$ and $\epsilon_R = 0$, the PS is reduced to the CPS case. To this end, we can write the minimum SR maximization problem as follows:

$$(P3) : \max_{\mathbf{w}, [\boldsymbol{\theta}]_b + \epsilon_R} \min_k \widehat{\text{SR}}_k(\mathbf{w}, \boldsymbol{\theta}), \quad (36a)$$

$$\text{s.t. } \sum_{k=1}^{\mathcal{K}} \|\mathbf{w}_k\|^2 \leq P_T, \quad (36b)$$

$$|e^{j(\lceil \boldsymbol{\theta} \rceil_b + \epsilon_R)}| = 1, \quad (36c)$$

$$\|\Delta \mathbf{u}_i\|_2 \leq \xi_i, i \in \{k, e\}, \forall k. \quad (36d)$$

Problem (P3) is a nonconvex problem due to the coupling between the beamforming vector and the IRS's PREs in the objective function, and the UMC (36c). However, problem (P3) is even more challenging due to the semi-infinite nonconvex

constraint (36d) that captures the imperfection of the CSI from IRS to the users/Eve. In addition to that, the imperfect CSI introduces PE into the IRS's PREs which makes the problem more challenging.

To tackle problem (P3), we first introduce slack variables to decompose the coupling of the beamforming vector and the IRS's PREs in the objective function. To this end, we first substitute (9) into (36a). Then we introduce slack variable z as the SR's lower bound, φ_k represents the minimum data rate, and μ_{k_e} represents the maximum eavesdropping rate of Eve. Thus, problem (P3) can be recast as:

$$(P3.1) : \max_{\mathbf{w}, [\boldsymbol{\theta}]_b + \epsilon_R} z, \quad (37a)$$

$$\text{s.t. } z \leq \varphi_k - \mu_{k_e}, \forall k, \quad (37b)$$

$$\varphi_k \leq \widehat{C}_k(\mathbf{w}, [\boldsymbol{\theta}]_b + \epsilon_R), \forall \|\Delta \mathbf{u}_k\|_2 \leq \xi_k, \forall k, \quad (37c)$$

$$\mu_{k_e} \geq \widehat{C}_e(\mathbf{w}, [\boldsymbol{\theta}]_b + \epsilon_R), \forall \|\Delta \mathbf{u}_e\|_2 \leq \xi_e, \forall k, \quad (37d)$$

$$(36b), (36c). \quad (37e)$$

One can notice that the constraint (36d) in problem (P3) has been embedded within the constraints (37c), and (37d) in problem (P3.1), since the channel estimation error $\Delta \mathbf{u}_i$ is embedded within the channel definition (4). Next, we employ the SCA technique and the \mathcal{S} -procedure to transform the semi-infinite nonconvex constraints (37c), and (37d) to finite LMIs. Then, we leverage a PCCP algorithm to tackle the UMC (36c).

1) *Sub-Problem for Optimizing the Beamforming Vectors*: To linearize the semi-infinite inequalities in (37c), we first substitute (11) into (37c), hence, (37c) can be expressed as:

$$2^{\varphi_k} - 1 \leq \frac{|(\mathbf{u}_k \Phi \mathbf{G}_{\text{AR}}) \mathbf{w}_k|^2}{\|(\mathbf{u}_k \Phi \mathbf{G}_{\text{AR}}) \mathbf{W}_{-k}\|^2 + \sigma_k}, \forall k. \quad (38)$$

By treating the interference plus noise signal as an auxiliary function $\boldsymbol{\beta} \triangleq [\beta_1, \dots, \beta_K]$, (38) can be expressed as,

$$|(\mathbf{u}_k \Phi \mathbf{G}_{\text{AR}}) \mathbf{w}_k|^2 \geq (2^{\varphi_k} - 1) \beta_k, \forall k, \quad (39a)$$

$$\|(\mathbf{u}_k \Phi \mathbf{G}_{\text{AR}}) \mathbf{W}_{-k}\|^2 + \sigma_k \leq \beta_k, \forall k. \quad (39b)$$

To circumvent the nonconvex semi-infinite inequalities in (39a), we replace the left-hand side of (39a) with their lower bounds by using the following Lemma.

Lemma 1: At iteration (ℓ) , let $\mathbf{w}^{(\ell)}$ and $[\boldsymbol{\theta}^{(\ell)}]_b$ be the optimal solution, then at the point $(\mathbf{w}^{(\ell)}, [\boldsymbol{\theta}^{(\ell)}]_b)$ we can express the linear lower bound of (39a) as in (41), where \mathbf{X}_k , is given in (40).

Proof: Please refer to Appendix B.

Next, by substituting (41) in (39a), and using (3a) and Lemma 1, the inequality in (39a) is reformulated as in (41), where $d_k \triangleq \hat{\mathbf{u}}_k \mathbf{X}_k \hat{\mathbf{u}}_k^H$.

To address the uncertainty of $\{\Delta \mathbf{u}_k\}$ in (41), we leverage the \mathcal{S} -procedure [16].

Lemma 2: (\mathcal{S} -procedure) For any Hermitian matrix $\mathbf{U}_i \in \mathbb{C}^{L \times L}$, vector $\mathbf{u}_i \in \mathbb{C}^{L \times 1}$, and scalar u_i , for $i = 0, \dots, Q$. A quadratic function of a variable x is defined as:

$$f_i(x) \triangleq x^H \mathbf{U}_i x + 2\Re\{\mathbf{u}_i^H x\} + u_i. \quad (42)$$

$$\mathbf{X}_k \triangleq \Phi \mathbf{G}_{\text{AR}} \mathbf{w}_k \mathbf{w}_k^{(\iota),H} \mathbf{G}_{\text{AR}}^H \Phi^{(\iota),H} + \Phi^{(\iota)} \mathbf{G}_{\text{AR}} \mathbf{w}_k^{(\iota)} \mathbf{w}_k^H \mathbf{G}_{\text{AR}}^H \Phi^{(\iota),H} - \Phi^{(\iota)} \mathbf{G}_{\text{AR}} \mathbf{w}_k^{(\iota)} \mathbf{w}_k^{(\iota),H} \mathbf{G}_{\text{AR}}^H \Phi^{(\iota),H}, \quad (40)$$

$$\Delta \mathbf{u}_k \mathbf{X}_k \Delta \mathbf{u}_k^H + 2\Re\{\mathbf{x}_k^H + \widehat{h}_{r,k}^H \mathbf{X}_k\} \Delta \mathbf{u}_k + d_k \geq (2^{\varphi_k} - 1)\beta_k, \forall \|\Delta \mathbf{u}\|_2 \leq \xi_k, \forall k. \quad (41)$$

The condition $f_0(x) \geq 0$ such that $f_i(x) \geq 0, i = 1, \dots, Q$, holds, if and only if there exists $\mathbf{n}_i \geq 0, i = 0, \dots, Q$, such that,

$$\begin{bmatrix} \mathbf{U}_0 & \mathbf{u}_0 \\ \mathbf{u}_0^H & u_0 \end{bmatrix} - \sum_{i=0}^Q \mathbf{n}_i \begin{bmatrix} \mathbf{U}_i & \mathbf{u}_i \\ \mathbf{u}_i^H & u_i \end{bmatrix} \succeq 0. \quad (43)$$

Using Lemma 2, we can transform (41) into its equivalent LMI as:

$$\begin{bmatrix} \varpi_k \mathbf{I}_M + \mathbf{X}_k & (\widehat{\mathbf{u}}_k \mathbf{X}_k)^H \\ (\widehat{\mathbf{u}}_k \mathbf{X}_k) & d_k - (2^{\varphi_k} - 1)\beta_k - \eta_k \xi_k^2 \end{bmatrix} \succeq 0, \forall k, \quad (44)$$

where $\boldsymbol{\eta} \triangleq [\eta_1, \dots, \eta_K]^T \geq 0$ are slack variables. Even though (39a) has been transformed into an LMI form, it is still nonconvex due to the nonconvexity nature of the term $2^{\varphi_k} \beta_k$. For that, we adopt the SCA technique [15] to convert the nonconvex constraint (44) to a convex approximation expression. Specifically, performing the first order Taylor approximation, the term $2^{\varphi_k} \beta_k$ can be upper bounded by:

$$(\beta_k (2^{\varphi_k}))^{ub} \triangleq ((\varphi_k - \varphi_k^{(\iota)}) (\beta_k^{(\iota)}) \ln 2 + \beta_k) 2^{\varphi_k^{(\iota)}}, \quad (45)$$

where $\varphi_k^{(\iota)}, \beta_k^{(\iota)}$ are the value of the variables φ_k, β_k at iteration (ι) in the SCA-based algorithm, respectively. Lastly, substituting (45) in (44), the LMIs in (44) can be expressed as:

$$\begin{bmatrix} \varpi_k \mathbf{I}_M + \mathbf{X}_k & (\widehat{\mathbf{u}}_k \mathbf{X}_k)^H \\ (\widehat{\mathbf{u}}_k \mathbf{X}_k) & d_k - (\beta_k (2^{\varphi_k}))^{ub} + \beta_k - \varpi_k \xi_k^2 \end{bmatrix} \succeq 0, \forall k. \quad (46)$$

Next, we tackle the uncertainties in (39b) using Schur's complement [28].

Lemma 3: (Schur's complement) For given matrices $\mathbf{U} \succeq 0, \mathbf{Y}$, and \mathbf{Z} , let a Hermitian matrix \mathbf{X} be defined as:

$$\mathbf{X} \triangleq \begin{bmatrix} \mathbf{Z} & \mathbf{Y}^H \\ \mathbf{Y} & \mathbf{U} \end{bmatrix}. \quad (47)$$

Then, $\mathbf{X} \succeq 0$ if and only if $\Delta \mathbf{U} \succeq 0$, where $\Delta \mathbf{U}$ is the Schur's complement define as $\Delta \mathbf{U} \triangleq \mathbf{Z} - \mathbf{Y}^H \mathbf{U}^{-1} \mathbf{Y}$.

Using Lemma (3), we can equivalently recast (39b) as:

$$\begin{bmatrix} \beta_k & \mathbf{t}_k^H \\ \mathbf{t}_k^H & \mathbf{I}_{K-1} \end{bmatrix} \succeq 0, \forall \|\Delta \mathbf{u}_k\|_2 \leq \xi_k, \forall k, \quad (48)$$

where,

$$\mathbf{t}_k \triangleq \left((\widehat{\mathbf{u}}_k^H \Phi \mathbf{G}_{\text{AR}}) \mathbf{W}_{-k} \right)^H, \\ \mathbf{W}_{-k} \triangleq [\mathbf{w}_1, \dots, \mathbf{w}_{k-1}, \mathbf{w}_{k+1}, \dots, \mathbf{w}_K].$$

Next, we use the Nemirovski's Lemma [29] to further handle (48).

Lemma 4: (Nemirovski's Lemma) For any Hermitian matrix \mathbf{A} , matrices \mathbf{B}, \mathbf{C} , and \mathbf{X} , and scalar t , the following LMI holds:

$$\mathbf{A} \succeq \mathbf{B}^H \mathbf{X} \mathbf{C} + \mathbf{C}^H \mathbf{X} \mathbf{B}, \text{ for } \|\mathbf{X}\| \leq t,$$

if and only if

$$\begin{bmatrix} \mathbf{A} - a \mathbf{C}^H \mathbf{C} & -t \mathbf{B}^H \\ -t \mathbf{B} & a \mathbf{I} \end{bmatrix} \succeq 0,$$

where a is a non-negative real number.

Using Lemma (4) and introducing the slack variable $\boldsymbol{\varkappa} \triangleq [\varkappa_1, \dots, \varkappa_k] \geq 0$, (48) is recast as:

$$\begin{bmatrix} B_{11,k} & \widehat{t}_k^H & \mathbf{0}_{1 \times M} \\ \widehat{t}_k & \mathbf{I}_{K-1} & \xi_{\mathbf{H}_k} (\Phi \mathbf{G}_{\text{AR}} \mathbf{W}_{-k})^H \\ \mathbf{0}_{M \times 1} & \xi_{\mathbf{H}_k} (\Phi \mathbf{G}_{\text{AR}} \mathbf{W}_{-k}) & \varkappa_k \mathbf{I}_M \end{bmatrix} \succeq 0, \quad (49)$$

where

$$B_{11,k} \triangleq \beta_k - \sigma_k - \varkappa_k, \\ \widehat{t}_k \triangleq ((\widehat{\mathbf{u}}_k \Phi \mathbf{G}_{\text{AR}}) \mathbf{W}_{-k})^H.$$

Next, we tackle (37d) by firstly substituting (11) in (37d), and then treating the interference plus noise signal in (37d) as an auxiliary function $\boldsymbol{\beta}_{e_k} \triangleq [\beta_{e_1}, \dots, \beta_{e_k}]$. We hence can recast (37d) as:

$$|(\mathbf{u}_e \Phi \mathbf{G}_{\text{AR}}) \mathbf{w}_k|^2 \leq (2^{\mu_{ke}} - 1) \beta_{ke}, \forall k, \quad (50a)$$

$$\|(\mathbf{u}_e \Phi \mathbf{G}_{\text{AR}}) \mathbf{W}_{-k}\|^2 + \sigma_e \geq \beta_{ke}, \quad \forall k. \quad (50b)$$

To tackle the uncertainties of $\{\Delta \mathbf{u}_e\}$ in constraints (50a) and (50b), we use a similar approach as in (39b). Hence, the equivalent LMIs of (50a) and (50b) are, respectively,

$$\begin{bmatrix} C_{e,k} & \widehat{c}_{ke}^H & \mathbf{0}_{1 \times M} \\ \widehat{c}_{ke} & 1 & \xi_e (\Phi \mathbf{G}_{\text{AR}} \mathbf{w}_k)^H \\ \mathbf{0}_{M \times 1} & \xi_e (\Phi \mathbf{G}_{\text{AR}} \mathbf{w}_k) & \vartheta_k \mathbf{I}_M \end{bmatrix} \succeq 0, \quad (51)$$

$$\begin{bmatrix} C_{11,k} & -\widehat{c}_{ke}^H & \mathbf{0}_{1 \times M} \\ -\widehat{c}_{ke} & \mathbf{I}_{K-1} & -\xi_e (\Phi \mathbf{G}_{\text{AR}} \mathbf{W}_{-k})^H \\ \mathbf{0}_{M \times 1} & -\xi_e (\Phi \mathbf{G}_{\text{AR}} \mathbf{W}_{-k}) & \varrho_k \mathbf{I}_M \end{bmatrix} \succeq 0, \quad (52)$$

where $\boldsymbol{\vartheta} \triangleq [\vartheta_1, \dots, \vartheta_K] \geq 0$ and $\boldsymbol{\varrho} \triangleq [\varrho_1, \dots, \varrho_K] \geq 0$ are a slack variables, and,

$$C_{e,k} \triangleq (\beta_{ke} (2^{\mu_{ke}}))^{ub} - \beta_{ke} - \vartheta_k,$$

$$(\beta_{ke} (2^{\mu_{ke}}))^{ub} \triangleq ((\mu_{ke} - \mu_{ke}^{(\iota)}) (\beta_{ke}^{(\iota)}) \ln 2 + \beta_{ke}) 2^{\mu_{ke}^{(\iota)}},$$

$$\widehat{c}_{ke} \triangleq ((\widehat{\mathbf{u}}_e^H \Phi \mathbf{G}_{\text{AR}}) \mathbf{W}_{-k})^H,$$

$$C_{11,k} \triangleq \beta_{ke} - \sigma_e - \varrho_k.$$

Eventually, reformulating problem (P3.2) with (46), (49), (51), and (52) yields the following optimization problem:

$$(P3.2) : \max_{\mathbf{w}} z, \quad (53a)$$

$$\text{s.t. } z \leq \varphi_k - \mu_{ke}, \quad \forall k, \quad (53b)$$

$$(46), (49), (51), (52), \quad (53c)$$

$$\boldsymbol{\omega} \geq 0, \boldsymbol{\varkappa} \geq 0, \boldsymbol{\vartheta} \geq 0, \boldsymbol{\varrho} \geq 0, \quad (53d)$$

$$(36b). \quad (53e)$$

At this point, all nonlinear constraints (37c) and (37d) have been linearized as LMIs (46), (49), (51), and (52); thus, problem (P3.2) is an SDP problem that can be efficiently solved using standard solvers, e.g., the interior point method or the CVX toolbox [25].

Algorithm 3 PCCP Algorithm to solve problem (P3.3)

- 1: **Initialize:** $(\mathbf{w}^{(1)}, \lfloor \boldsymbol{\theta}^{(1)} \rfloor_b + \epsilon_R)$, the maximum penalty factor o_{\max} , the scaling factor $\nu \geq 1$, convergence tolerance ϵ_{t_1} and ϵ_{t_2} , maximum number of iterations ι_{\max} , and Set $\iota = 1$.
 - 2: **Repeat**
 - 3: **For** $\iota \leq \iota_{\max}$
 - 4: Solve problem (P3.3) to obtain $\lfloor \boldsymbol{\theta}_n^{(\iota+1)} \rfloor_b$;
 - 5: **end if** $\left\| e^{(j\lfloor \boldsymbol{\theta}_n^{(\iota)} \rfloor_b)} - e^{(j\lfloor \boldsymbol{\theta}_n^{(\iota+1)} \rfloor_b)} \right\|_1 \leq \epsilon_{t_1}$ and $Q \leq \epsilon_{t_2}$.
 - 6: **else**
 - 7: Obtain $o^{(\iota+1)} = \min\{\nu o^{(\iota)}, o_{\max}\}$;
 - 8: Update $\iota = \iota + 1$;
 - 9: **else**
 - 10: define a new $\lfloor \boldsymbol{\theta}^{(1+\epsilon_R)} \rfloor_b$, set $\nu > 1$ and $\iota = 0$.
 - 11: **Output** the feasible solution $\boldsymbol{\theta}^* = \lfloor \boldsymbol{\theta}^{(\iota)} \rfloor_b + \epsilon_R$.
-

2) *Sub-Problem for Optimizing the PREs:* For a given \mathbf{w} , we aim to find $\lfloor \boldsymbol{\theta}^{(\iota+1)} \rfloor_b$ such that, $\text{SR}_k(\mathbf{w}_k^{(\iota+1)}, \lfloor \boldsymbol{\theta}^{(\iota+1)} \rfloor_b) > \text{SR}_k(\mathbf{w}_k^{(\iota+1)}, \lfloor \boldsymbol{\theta}^{(\iota)} \rfloor_b)$. Similar to the analysis in the previous section, we can express (37c) and (37d) with their equivalent LMIs (46), (49), (51) and (52), respectively.

To tackle the UMC (36c), we leverage the PCCP method [17]. The PCCP's main idea is to add slack variables to relax the problem so that if the UMC is violated, we then can penalize the sum of violations. The converged PCCP solution is an approximate first-order optimal solution of the original problem [17].

To apply the PCCP method, we first introduce an auxiliary variable set $\mathbf{d} \triangleq \{d_n | n \in N\}$ satisfying $d_n \triangleq |e^{(j\lfloor \boldsymbol{\theta}_n^{(\iota)} \rfloor_b)}| * |e^{(j\lfloor \boldsymbol{\theta}_n^{(\iota+1)} \rfloor_b)}|$. Then, (36c) can be expressed as $d_n \leq |e^{(j\lfloor \boldsymbol{\theta}_n^{(\iota)} \rfloor_b)}| * |e^{(j\lfloor \boldsymbol{\theta}_n^{(\iota+1)} \rfloor_b)}| \leq d_n$. The nonconvex part $d_n \leq |e^{(j\lfloor \boldsymbol{\theta}_n^{(\iota)} \rfloor_b)}| * |e^{(j\lfloor \boldsymbol{\theta}_n^{(\iota+1)} \rfloor_b)}|$ can be approximated by $d_n \leq 2\Re\{|e^{(j\lfloor \boldsymbol{\theta}_n^{(\iota)} \rfloor_b)}| * |e^{(j\lfloor \boldsymbol{\theta}_n^{(\iota+1)} \rfloor_b)}| - |e^{(j\lfloor \boldsymbol{\theta}_n^{(\iota)} \rfloor_b)}| * |e^{(j\lfloor \boldsymbol{\theta}_n^{(\iota+1)} \rfloor_b)}|\}$. Following the PCCP framework, we penalize the objective function (37a), hence, problem (P3.1) can be recast as:

$$(P3.3) : \max_{\boldsymbol{\theta}} z - oQ, \quad (54a)$$

$$\text{s.t.} \quad (46), (49), (51), (52), \quad (54b)$$

$$|e^{(j\lfloor \boldsymbol{\theta}_n^{(\iota)} \rfloor_b)}| * |e^{(j\lfloor \boldsymbol{\theta}_n^{(\iota+1)} \rfloor_b)}| \leq d_n + c_n, \quad (54c)$$

$$d_n - \hat{c}_n \leq 2\Re\left\{|e^{(j\lfloor \boldsymbol{\theta}_n^{(\iota)} \rfloor_b)}| * |e^{(j\lfloor \boldsymbol{\theta}_n^{(\iota+1)} \rfloor_b)}|\right\} - |e^{(j\lfloor \boldsymbol{\theta}_n^{(\iota)} \rfloor_b)}| * |e^{(j\lfloor \boldsymbol{\theta}_n^{(\iota+1)} \rfloor_b)}|, \quad (54d)$$

$$d_n \geq 0, \quad \forall n \in N. \quad (54e)$$

where $Q \triangleq \sum_{n=1}^N c_n + \hat{c}_n$ is the penalty term, $\mathbf{c} \triangleq \{c_n, \hat{c}_n\}$ is the slack variable imposed over the modulus constraint (36c), and o is the regularization factor. The regularization factor is imposed to control the UMC constraint (36c) by scaling the penalty term Q .

Problem (P3.3) is an SDP problem that can be solved by the CVX toolbox. Unlike the semi-definite relaxation (SDR) method, which is the conventional method to tackle UMC, the PCCP method is guaranteed to find a feasible point for problem (P3.3) [30]. The PCCP algorithm to solve problem (P3.3) is described in Algorithm 3. The following points are emphasized from Algorithm 3:

- (a) We invoke o_{\max} to avoid numerical complications if o grows too large [31];
- (b) The stopping criteria $Q \leq \epsilon_{t_2}$ guarantees the UMC (36c) when ϵ_{t_2} is small [10];

Algorithm 4 Proposed AO Algorithm for Solving Problem (P3)

- 1: **Initialize:** $(\mathbf{w}^{(1)}, \lfloor \boldsymbol{\theta}^{(1)} \rfloor_b + \epsilon_R)$, $\iota = 1$, and convergence tolerance $\epsilon_t > 0$.
 - 2: **Repeat**
 - 3: Update $\mathbf{w}^{(\iota+1)}$ by solving (P3.2), and $\lfloor \boldsymbol{\theta}_n^{(\iota+1)} \rfloor_b$ by solving problem (P3.2);
 - 4: **if** $\frac{\min_k \text{SR}_k(\mathbf{w}^{(\iota+1)}, \lfloor \boldsymbol{\theta}_n^{(\iota+1)} \rfloor_b + \epsilon_R) - \min_k \text{SR}_k(\mathbf{w}^{(\iota)}, \lfloor \boldsymbol{\theta}^{(\iota)} \rfloor_b + \epsilon_R)}{\min_k \text{SR}_k(\mathbf{w}^{(\iota)}, \lfloor \boldsymbol{\theta}^{(\iota)} \rfloor_b + \epsilon_R)} \leq \epsilon_t$.
 - 5: **Then** $\lfloor \boldsymbol{\theta}^{(\iota)} \rfloor_b \leftarrow \lfloor \boldsymbol{\theta}_n^{(\iota+1)} \rfloor_b$, $\mathbf{w}^{(\iota)} \leftarrow \mathbf{w}^{(\iota+1)}$ and terminate.
 - 6: **Otherwise** $\iota \leftarrow \iota + 1$ and continue.
 - 7: **Output** $(\mathbf{w}_k^{(\iota)}, \lfloor \boldsymbol{\theta}^{(\iota)} \rfloor_b + \epsilon_R)$.
-

(c) The convergence of Algorithm 3 is controlled by $\left\| e^{(j\lfloor \boldsymbol{\theta}^{(\iota)} \rfloor_b)} - e^{(j\lfloor \boldsymbol{\theta}^{(\iota-1)} \rfloor_b)} \right\|_1 \leq \epsilon_{t_1}$.

Algorithm 4 demonstrates the AO algorithm to solve problem (P3), whose converges to at least a locally optimal solution of (P3), which can be proved in the following theorem.

Theorem 3: The AO Algorithm 4 generates a locally optimal solution for problem (P3).

Proof: See Appendix C.

3) *Complexity Analysis:* Since convex problems (P2.2) and (P2.3) involve linear constraints and LMIs (46), (49), (51), (52), they can be solved by the interior point method [25]. Thus, Algorithm 4 complexity is defined by its worst-case runtime and the number of operations [10]. For problem (P2.2), the number of variables is $c \triangleq 2M$, the size of (46) is $a_1 \triangleq MN + M + 1$, the size of (49), and (52) is $a_2 \triangleq 2M + 1$, and the size of (51) is $a_3 \triangleq 2M + 1$. Thus, the complexity of solving problems (P2.2) and (P2.3), respectively,

$$\mathcal{O}_{\mathbf{w}} \triangleq \mathcal{O}\left\{\sqrt{b_1 + 2(c)}(c^2 + cb_2 + b_3 + (c+1)^2)\right\}, \quad (55)$$

$$\mathcal{O}_{\Phi} \triangleq \mathcal{O}\left\{\sqrt{b_1 + 4N(2N)}(4N^2 + 2Nb_2 + b_3 + 4NM)\right\}, \quad (56)$$

where,

$$b_1 \triangleq \sum_k^{\mathcal{K}} (a_1 + a_2) + 2k(a_2 + a_3) + (k-2)(a_1 + a_3),$$

$$b_2 \triangleq \sum_k^{\mathcal{K}} (a_1^2 + a_2^2) + 2k(a_2^2 + a_3^2) + (k-2)(a_1^2 + a_3^2),$$

$$b_3 \triangleq \sum_k^{\mathcal{K}} (a_1^3 + a_2^3) + 2k(a_2^3 + a_3^3) + (k-2)(a_1^3 + a_3^3).$$

B. SSR maximization under imperfect CSI

Previous research such as [8] has considered a similar problem with the presence of a direct link between Alice and the users and Eve. The SSR maximization problem under imperfect CSI from IRS to users/Eve can be formally formulated as:

$$(P4) : \max_{\mathbf{w}, \boldsymbol{\theta}} \sum_{k=1}^{\mathcal{K}} \widehat{\text{SR}}_k(\mathbf{w}, \boldsymbol{\theta}), \quad (57a)$$

$$\text{s.t.} \quad (36b), (36c), (36d). \quad (57b)$$

Similar to (P3), problem (P4) is a nonconvex problem due to the coupling between the beamforming vector and the IRS's PREs within the objective function, and the UMC (36c).

To tackle problem (P4), we first substitute (9) in (57a), and introduce the slack variables \tilde{z} as lower bound of the

Algorithm 5 Proposed AO Algorithm for Solving Problem (P4)

- 1: **Initialize:** $(\mathbf{w}^{(1)}, [\boldsymbol{\theta}^{(1)}]_{b+\epsilon_R})$, convergence tolerance $\epsilon_t > 0$, and Set $\iota = 1$.
 - 2: **Repeat**
 - 3: Update $\mathbf{w}^{(\iota+1)}$ by solving problem P4.2, and $[\boldsymbol{\theta}_n^{(\iota+1)}]_b + \epsilon_R$ by solving problem P4.3;
 - 4: **if** $\frac{\sum_{k=1}^K \text{SR}_k(\mathbf{w}^{(\iota+1)}, [\boldsymbol{\theta}_n^{(\iota+1)}]_{b+\epsilon_R}) - \sum_{k=1}^K \text{SR}_k(\mathbf{w}^{(\iota)}, [\boldsymbol{\theta}^{(\iota)}]_{b+\epsilon_R})}{\sum_{k=1}^K \text{SR}_k(\mathbf{w}^{(\iota)}, [\boldsymbol{\theta}^{(\iota)}]_{b+\epsilon_R})} \leq \epsilon_t$.
 - 5: **Then** $[\boldsymbol{\theta}^{(\iota)}]_b \leftarrow [\boldsymbol{\theta}_n^{(\iota+1)}]_b$, $\mathbf{w}^{(\iota)} \leftarrow \mathbf{w}^{(\iota+1)}$ and terminate.
 - 6: **Otherwise** $\iota \leftarrow \iota + 1$ and continue.
 - 7: **Output** $(\mathbf{w}_k^{(\iota)}, [\boldsymbol{\theta}^{(\iota)}]_{b+\epsilon_R})$.
-

SSR, $\tilde{\varphi}_k$ and $\tilde{\mu}_{k_e}$ as the minimum data rate, and the maximum eavesdropping rate of Eve, respectively, hence, problem (P4) can be recast as:

$$(P4.1) : \max_{\mathbf{w}, [\boldsymbol{\theta}]_b} \tilde{z}, \quad (58a)$$

$$\text{s.t.} \quad \tilde{z} \leq \sum_{k=1}^K (\tilde{\varphi}_k - \tilde{\mu}_{k_e}), \forall k, \quad (58b)$$

$$\tilde{\varphi}_k \leq \hat{C}_k(\mathbf{w}, [\boldsymbol{\theta}]_b + \epsilon_R), \forall \|\Delta \mathbf{u}_k\|_2 \leq \xi_k, \quad (58c)$$

$$\tilde{\mu}_{k_e} \geq \hat{C}_e(\mathbf{w}, [\boldsymbol{\theta}]_b + \epsilon_R), \forall \|\Delta \mathbf{u}_e\|_2 \leq \xi_e, \quad (58d)$$

$$(36b), (36c). \quad (58e)$$

To tackle problem (P4.1), we use a similar approach that dealt with problem (P3.1).

1) *Sub-Problem for Optimizing the Beamforming Vectors:*

Similar to the analysis to linearize (39a) and (39b) in section IV. First, we introduce an auxiliary variable \tilde{z} as the lower bound of the SSR. Then, we express (58c) and (58d) with their equivalent LMIs (46), (49), (51) and (52), respectively. Thus, problem (P4.1) can be recast as:

$$(P4.2) : \max_{\mathbf{w}, \boldsymbol{\theta}} \tilde{z}, \quad (59a)$$

$$\text{s.t.} \quad \tilde{z} \leq \sum_{k=1}^K (\tilde{\varphi}_k - \tilde{\mu}_{k_e}), \forall k, \quad (59b)$$

$$(36b), (46), (49), (51), (52), (53d). \quad (59c)$$

Problem (P4.2) is a convex problem that can be solved using the CVX toolbox.

2) *Sub-Problem for Optimizing the PREs:* Similarly, we can express (58c) and (58d) with their equivalent LMIs (46), (49), (51) and (52), respectively. To tackle the UMC (36c), we use the PCCP method as described in Algorithm 3. Finally, the steps to solve problem (P4) are described in Algorithm 5.

Theorem 4: The obtained solution by Algorithm 5 is a locally optimal solution for problem P4.

Proof: See Appendix C.

3) *Complexity Analysis:* The complexity analysis of Algorithm 5 is similar to Algorithm 4. Hence, the complexity of problem P4 is expressed in (55) and (56).

V. DEALING WITH EVE'S UNKNOWN CSI

In this case, we assume that Alice can't obtain Eve's CSI (even just the imperfect CSI). To provide secure communications for *all users*, we propose to optimize a minimum transmit power P_T subject to a quality of service (QoS) constraint (i.e. $\gamma_k \geq \gamma_e$) to allow us to use the residual power available at Alice as AN so as to decrease the SINR at Eve γ_e . Unlike other research [32], [33], that only deals with a single user and assumes perfect CSI under IRS' PREs CPS, we address the

Algorithm 6 Proposed AO Algorithm for Solving Problem (P5)

- 1: **Initialize:** $(\mathbf{w}^{(1)}, [\boldsymbol{\theta}^{(1)}]_{b+\epsilon_R})$, convergence tolerance $\epsilon_t > 0$, and Set $\iota = 1$.
 - 2: **Repeat**
 - 3: Update $\mathbf{w}^{(\iota+1)}$ by solving problem (P5.2), and $[\boldsymbol{\theta}_n^{(\iota+1)}]_b$ by solving problem (P5.3);
 - 4: **if** $\frac{\sum_{k=1}^K \|\mathbf{w}^{(\iota+1)}\|^2 - \sum_{k=1}^K \|\mathbf{w}^{(\iota)}\|^2}{\sum_k \|\mathbf{w}^{(\iota)}\|^2} \leq \epsilon_t$.
 - 5: **Then** $[\boldsymbol{\theta}^{(\iota)}]_b \leftarrow [\boldsymbol{\theta}_n^{(\iota+1)}]_b$, $\mathbf{w}^{(\iota)} \leftarrow \mathbf{w}^{(\iota+1)}$ and terminate.
 - 6: **Otherwise** $\iota \leftarrow \iota + 1$ and continue.
 - 7: **Output** $(\mathbf{w}_k^{(\iota)}, [\boldsymbol{\theta}^{(\iota)}]_{b+\epsilon_R})$.
-

power minimization problem under the multi-users settings, where only partial users' CSI is available, and the IRS's PREs are modeled by the QPS and suffer PSE due to the imperfect CSI. To this end, we can express the total transmit power P_{tot} as follows:

$$P_{tot} \triangleq P_T + P_J, \quad (60)$$

where the residual power $P_J \triangleq \sum_{k=1}^K \mathbf{E}\{\|\mathbf{V}\mathbf{r}\|^2\}$ is used as AN, and $\mathbf{V}\mathbf{r}$ is the AN vector, while $\mathbf{V} \in \mathbb{C}^{M \times M-1}$ is the null space of the user's channel with $\mathbf{h}_k([\boldsymbol{\theta}]_b + \epsilon_R)\mathbf{V} = 0$, and $\mathbf{r} \in \mathbb{C}^{M-1}$ is a random vector whose elements are independent Gaussian random variables with mean 0 and variance $\sigma_r \triangleq \frac{P_J}{M-1}$. Hence, we can express the SINR at user- k as in (6), and Eve's eavesdropping rate as:

$$\gamma_e(\mathbf{w}, [\boldsymbol{\theta}]_b + \epsilon_R) \triangleq \frac{|\hat{\mathbf{h}}_e([\boldsymbol{\theta}]_b + \epsilon_R)\mathbf{w}_k|^2}{\hat{\rho}_e + |\hat{\mathbf{h}}_e([\boldsymbol{\theta}]_b + \epsilon_R)\mathbf{V}\mathbf{r}|^2}. \quad (61)$$

To that end, we can formulate the problem as:

$$(P5) : \min_{\mathbf{w}, \boldsymbol{\theta}} P_T, \quad (62a)$$

$$\text{s.t.} \quad \gamma_k(\mathbf{w}, [\boldsymbol{\theta}]_b + \epsilon_R) \geq \gamma\sigma_k, \quad (62b)$$

$$(36b), (36c), (36d). \quad (62c)$$

where γ represents the QoS constraint at user- k . Due to the coupling of \mathbf{w} and $\boldsymbol{\theta}$ in (62b), problem (P3) is a nonconvex problem.

1) *Sub-Problem for Optimizing the Beamforming Vectors:* similar to the previous sections, we propose an AO method to tackle problem (P5), by designing the beamform vector \mathbf{w} with fixed $\boldsymbol{\theta}$. Hence, problem (P5) can be recast as:

$$(P5.1) : \min_{\mathbf{w}} P_T, \quad (63a)$$

$$\text{s.t.} \quad |(\mathbf{u}_k \Phi \mathbf{G}_{AR})\mathbf{w}_k|^2 \geq (2^{\gamma_k} - 1)\hat{\beta}_k, \forall k, \quad (63b)$$

$$\|(\mathbf{u}_k \Phi \mathbf{G}_{AR})\mathbf{W}_{-k}\|^2 + \sigma_k \leq \hat{\beta}_k, \forall k, \quad (63c)$$

$$(36b). \quad (63d)$$

where $\hat{\beta} \triangleq [\hat{\beta}_1, \dots, \hat{\beta}_K]$ is an auxiliary function. Similar to the analysis to linearize (39a) and (39b) in section IV, we can express (63b) and (63c) with their equivalent LMIs (46), (49), (51) and (52), respectively. Thus, problem (P5.1) can be recast as:

$$(P5.2) : \min_{\mathbf{w}} P_T, \quad (64a)$$

$$\text{s.t.} \quad (36b), (46), (49), (51), (52), (53d). \quad (64b)$$

Problem (P5.2) is a convex problem that can be solved using the CVX toolbox.

TABLE I: Numerical Parameters

Parameter	Numerical Value
Noise power density (σ_i)	-174 dBm/Hz
Alice Transmission power (P)	20 dBm
Antennas' Gain (G_A) and (G_{IRS})	5 dBi
PS bits (b)	3
the convergence tolerance ϵ_t	10^{-3}
simulation initial settings	$\beta_k^{(1)} = 1, \beta_{k_e}^{(1)} = 1, o^{(1)} = 10,$ $\alpha_{\max} = 30, \delta_k = \delta_e = 0.02.$

2) *Sub-Problem for Optimizing the PREs*: Similarly, we aim to find $[\theta^{(\ell+1)}]_b$ that minimizes P_T while meeting the QoS constraint (62b). This problem is a search problem to find any feasible $[\theta]_b$ satisfying the QoS (62b) and the UMC constraint (36c), where the obtained result can be the optimal solution. Hence, one can use the residual power (60) and the PCCP algorithm as described in Algorithm 3 to find the optimal $[\theta]_b$.

Finally, the algorithm to solve problem (P5.3) is described in Algorithm 6.

Theorem 5: The obtained solution by the AO Algorithm 6 is a locally optimal solution for problem (P5).

Proof: See Appendix C.

3) *Complexity Analysis*: Algorithm 6 involves linear constraints and LMIs (46), (49), (51), (52), hence, its complexity is similar to Algorithm 4, which can be expressed as in (55) and (56).

VI. SIMULATIONS RESULTS

In this section, we perform extensive simulations to evaluate the performance of the proposed approach and algorithms. The results are obtained using the MATLAB and CVX toolboxes. Alice is located at (15, 0, 15), the IRS is located at (0, 25, 40), and the users are randomly distributed to the right of Alice over a $(60m \times 60m)$ area. The Eve (e.g., a compromised legitimate user) is randomly located in $(60m \times 60m)$ outside the user's area. Note that if Eve is too close to one of the users, it is mostly impossible to guarantee the positive SR for all users [34]. In this case, other methods, e.g., encryption or friendly jamming, can provide users' secrecy.

The Alice-to-users/Eve direct path factor is $\beta_{A_i} \triangleq G_A - 35.9 - 22 \log_{10}(d_i)$, $i \in \{k, e\}$, where d_i is the distance between Alice and the users/Eve, while G_A is Alice antenna gain. The Alice-to-IRS direct path loss factor is $\beta_{AR} \triangleq G_A + G_{IRS} - 35.9 - 22 \log_{10}(d_{AR})$ in dB, where d_{AR} is the distance between Alice and the IRS in meters, and G_{IRS} is the IRS elements' antenna gain [35]. The path loss factor from the IRS to the users and the Eve is $\beta_{Ri} \triangleq G_{IRS} - 33.05 - 30 \log_{10}(d_{Ri})$ dB, for $i \in \{k, e\}$, d_{Ri} is the distance between the IRS and the users and Eve in meters. The spatial correlation matrix is $[R_{Ri}]_{l,\bar{l}} \triangleq \exp(j\pi(l - \bar{l}) \sin \hat{\nu} \sin \hat{\kappa})$ for $i \in \{k, e\}$, where $\hat{\kappa}$ is the elevation angle and $\hat{\nu}$ is the azimuth angle. The elements of the Alice-to-IRS channel are generated by $[G_{AR}]_{a,b} \triangleq \exp(j\pi((b-1) \sin \bar{\Theta}_b \sin \bar{\vartheta}_b + (a-1) \sin(\Theta_n) \sin(\vartheta_b)))$, where $\Theta_n \in (0, 2\pi)$, $\vartheta_n \in (0, 2\pi)$, and $\bar{\Theta}_n \triangleq \pi - \Theta_n$, and $\bar{\vartheta}_n \triangleq \pi + \vartheta_n$ [20]. The small-scale fading channel gain \mathbf{u}_i for $i \in \{k, e\}$ is modeled as a Rician fading channel with K-factor=3.

We define the CSI error bounds as $\xi_i \triangleq \delta_i \|\hat{\mathbf{u}}_i\|_2, \forall k$, where $\delta_i \in [0, 1], i \in \{k, e\}$ is the relative amount of CSI uncertainty. When $\delta = 0$, Alice can obtain the perfect CSI of the IRS to users/Eve reflected channel. Unless stated otherwise, the simulation parameters are defined in Table I. Lastly, we multiply the results by $\log_2(e)$ to convert them to bps/Hz.

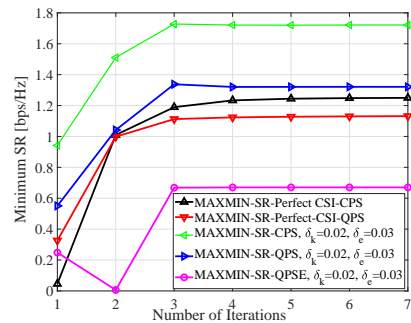


Fig. 2: Convergence rate of the Max-Min algorithm with $M = 10, \mathcal{K} = 6, N = 16$.

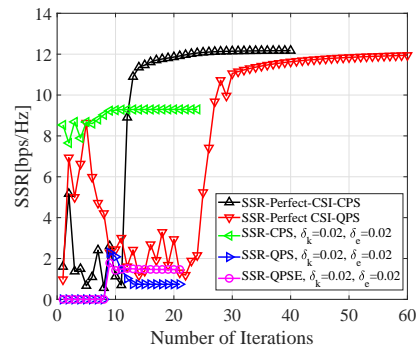


Fig. 3: Convergence rate of SSR maximization with $M = 10, \mathcal{K} = 6, N = 16$.

Fig. 2 illustrates the convergence rate of the Max-Min algorithms under the perfect and imperfect CSI for the CPS, the QPS, and the QPSE cases with $M = 10, \mathcal{K} = 6$, and $N = 16$. All algorithms achieve convergence within a few iterations. The obtained results show the robustness of the proposed algorithm, even when the IRS's PREs PS are subject to phase error and CSI uncertainty, the system still can achieve secrecy for *all users*. The SSR counterpart convergence rate is shown in Fig. 3. One can notice the oscillation at the beginning of the convergence curve, which occurs when the SSR algorithm is trying to provide secrecy to *all users*. It can be noticed that the convergence is unreachable until the algorithm drops the users with zero secrecy, which is visible in all cases. The results show that the SSR algorithm suffers from the PS error more than the Max-Min algorithm.

Fig. 4 shows the users' SR distribution with $M = 10, \mathcal{K} = 6$, and $N = 16$, under the Max-Min algorithms for perfect and imperfect CSI cases with CPS, QPS, and QPSE. The CPS achieves the highest fairness between the three cases, which is expected. However, both the QPS and QPSE cases achieved secrecy for *all users* with less fairness compared to the CPS case, and the QPSE case which has the least fairness in SR among the three cases. However, when the IRS's PREs are not practically optimized, the algorithms fail to achieve secrecy fairness among the users. The results demonstrate the importance of properly optimizing the IRS's PREs to achieve secrecy fairness. The users' SR under the SSR maximization counterparts is shown in Fig. 5. The SSR maximization algorithms fail to provide secrecy to *all users* and focus most of the transmission power toward the users with better channels.

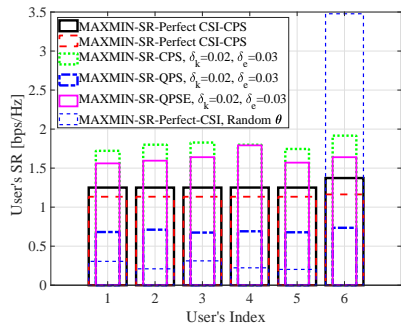


Fig. 4: Users' SR with $M = 10$, $\mathcal{K} = 6$, $N = 16$.

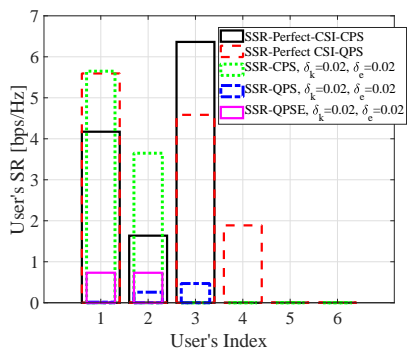


Fig. 5: Users' SR with $M = 10$, $\mathcal{K} = 7$, $N = 16$.

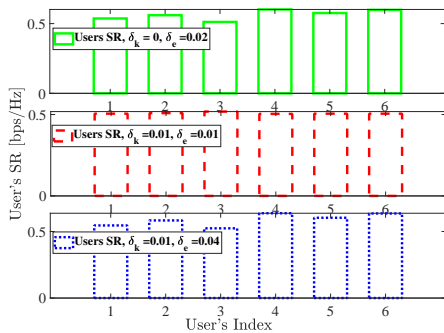


Fig. 6: Users' SR with with $M = 10$, $\mathcal{K} = 6$, $N = 16$.

Fig. 6 depicts the users' SR under different values of the IRS to the users/Eve imperfect CSI. The Max-Min algorithm achieves secrecy fairness in all the cases, even when Eve's reflected channel has higher uncertainty than the users' reflected channel.

To evaluate the degree of fairness in the proposed algorithms under imperfect CSI using the Jain's index, Jain's index is defined as, $\text{Jain's Index} = \frac{(\sum_{k=1}^{\mathcal{K}} \text{SR}_k(\mathbf{w}, \boldsymbol{\theta}))^2}{\mathcal{K} \sum_{k=1}^{\mathcal{K}} (\text{SR}_k(\mathbf{w}, \boldsymbol{\theta}))^2}$, and it is bounded in $[1/\mathcal{K}, 1]$, where the higher value indicates a better fairness [36]. Fig. 7 depicts Jain's index while varying the number of Alice's antennas M , with $M = 10$, $\mathcal{K} = 6$, and $N = 16$. The proposed Max-Min algorithm achieves almost one for the Jain's index in the CPS/QPS/QPSE cases. As expected, the SSR counterpart achieves low fairness between the user since it favors most of the transmission power P_T towards the users with a better channel while discarding other users, which matches the previous results.

Fig. 8 shows the Jain's index against the relative amount of

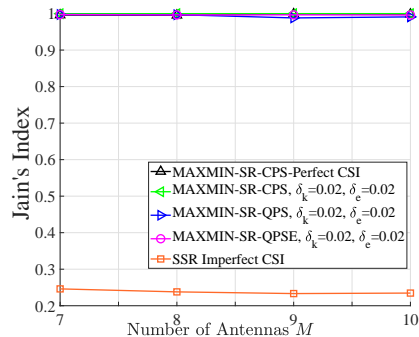


Fig. 7: Jain's Index Vs. the number of Alice's antennas M , with $\mathcal{K} = 4$, $N = 16$.

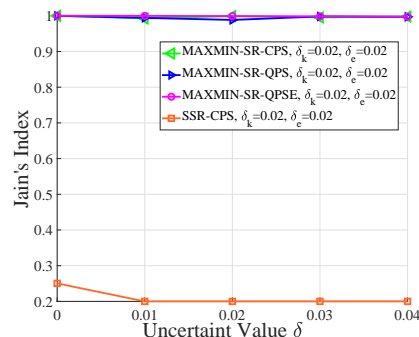


Fig. 8: Jain's Index Vs. the uncertainty level $\delta_k = \delta_e$ with $M = 10$, $\mathcal{K} = 5$, $N = 16$.

CSI uncertainty δ . The Max-Min algorithm achieves almost one in all cases CPS/QPS/QPSE, while the SSR counterpart has nearly zero. The results demonstrate the Max-Min algorithm's robustness even when the phase error is introduced at high uncertainty CSI for the users and Eve counterpart.

Fig. 9 illustrates the convergence rate of Algorithm 6 with the QPS and the QPSE cases. The algorithm converges within a few iterations. Fig. 10 shows the users' SR distribution with $M = 10$, $\mathcal{K} = 5$, and $N = 16$, under the power minimization algorithm for imperfect CSI case with QPS, and QPSE. All users have achieved secrecy while maintain the minimum QoS constraint $\gamma_k = 0.5$ [dB], which demonstrates the robustness of the proposed algorithm even with QPSE and the users' imperfect CSI introduced, while Eve's CSI is unknown to Alice.

Lastly, Fig. 11 depicts the minimum transmit power P_T against the minimum user's SINR γ_k . The minimum power increase with γ_k as expected, since the system requires more transmit power to achieve higher users' SINR. The results show that the system will require higher transmit power to achieve secrecy for all users with increasing \mathcal{K} , and it can achieve secrecy even when the PREs are subject to the QPSE.

VII. CONCLUSIONS

In this paper, we proposed a framework to achieve secure communications for all the users in a low resolution IRS-aided system with the presence of an eavesdropper under both perfect and imperfect CSI. Specifically, through linearization and different non-convex optimization techniques, we designed computationally efficient algorithms to maximize the minimum SR among all users under both perfect and imperfect CSI from IRS to the users and the eavesdropper, and minimize

$$\ln |I_n + [\mathbf{A}]^2(\mathbf{F})^{-1}| \geq \ln |I_n + [\hat{\Lambda}]^2(\hat{\mathbf{F}})^{-1}| - \langle [\hat{\Lambda}]^2(\hat{\mathbf{F}})^{-1} \rangle + 2\Re\{\langle \hat{\Lambda}^H(\hat{\mathbf{F}})^{-1} \mathbf{A} \rangle\} - \langle (\hat{\mathbf{F}})^{-1} - (\hat{\mathbf{F}} + [\hat{\Lambda}]^2)^{-1}, [\mathbf{A}]^2 + \mathbf{F} \rangle, \quad (65)$$

$$\ln(1 + \sum_{i=1}^l |z_i|^2) \geq \ln(1 + \sum_{i=1}^l |\bar{z}_i|^2) - \sum_{i=1}^l |\bar{z}_i|^2 + \sum_{i=1}^l 2\Re\{\bar{z}_i^* z_i\} - \frac{\sum_{i=1}^l |\bar{z}_i|^2 (1 + \sum_{i=1}^l |z_i|^2)}{1 + \sum_{i=1}^l |\bar{z}_i|^2}. \quad (66)$$

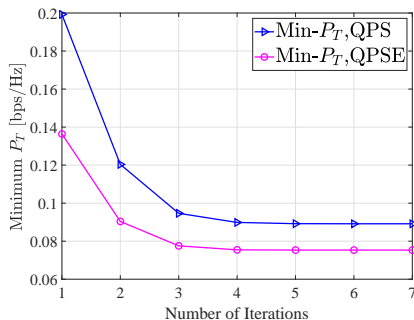


Fig. 9: Convergence rate of the Min P_T algorithm with $M = 10$, $\mathcal{K} = 5$, $N = 16$, $b = 3$, $\delta_k = 0.01$, $\gamma_k = 0.5$ [dB].

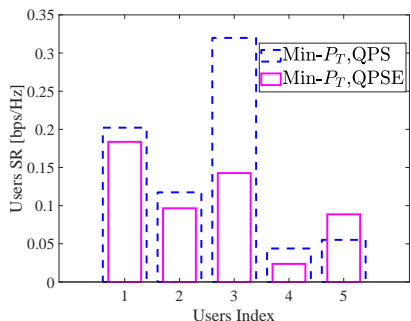


Fig. 10: Users' SR with $M = 10$, $\mathcal{K} = 5$, $N = 16$, $b = 3$, $\delta_k = 0.01$, $\gamma_k = 0.5$ [dB].

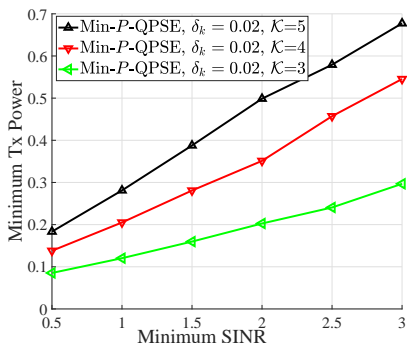


Fig. 11: Min-Tx-Power Vs. the minimum users' SINR γ_k with $M = 10$, $N = 25$, $b = 3$.

the transmit power subject to minimum SR constraints, where the IRS's PREs are modeled by quantized phase shift (QPS) and affected by phase shift error (PSE). Extensive simulations results showed that the Max-Min algorithm can provide secure communications for all the users even with only imperfect CSI. In the future, one can consider a multi-hop scenario with the

joint coding over multiple IRSs or distributed beamforming, similar to the cooperative MIMO setting [?].

APPENDIX A

PROOF OF THEOREM 1

First we prove that the sequence $\text{SR}_k(\mathbf{w}^{(\ell+1)}, [\boldsymbol{\theta}_n^{(\ell+1)}]_b + \epsilon_R)$ is non decreasing for all k , i.e. $\text{SR}_k(\mathbf{w}^{(\ell+1)}, [\boldsymbol{\theta}_n^{(\ell+1)}]_b) \geq \text{SR}_k(\mathbf{w}^{(\ell)}, \boldsymbol{\theta}^{(\ell)})$ for all $\ell > 0$. To that end, with the aid of the CVX solver, we obtain $\mathbf{w}^{(\ell+1)}$ by solving problem (P1.2). CVX solver is guaranteed to find the optimal solution. Thus, we have $\text{SR}_k(\mathbf{w}^{(\ell+1)}, [\boldsymbol{\theta}]_b + \epsilon_R) > \text{SR}_k(\mathbf{w}^{(\ell)}, \boldsymbol{\theta})$ for all k . Next, from (P1.3), we obtain $[\boldsymbol{\theta}_n^{(\ell+1)}]_b + \epsilon_R$, where we have $\text{SR}_k(\mathbf{w}, [\boldsymbol{\theta}_n^{(\ell+1)}]_b + \epsilon_R) > \text{SR}_k(\mathbf{w}, [\boldsymbol{\theta}^{(\ell)}]_b + \epsilon_R)$ as stated before.

Hence, by combining the solutions we obtain

$$\text{SR}_k(\mathbf{w}^{(\ell+1)}, [\boldsymbol{\theta}_n^{(\ell+1)}]_b + \epsilon_R) > \text{SR}_k(\mathbf{w}^{(\ell)}, [\boldsymbol{\theta}^{(\ell)}]_b + \epsilon_R), \quad (67)$$

hence, the optimal sequence $\{(\mathbf{w}^{(\ell+1)}, [\boldsymbol{\theta}_n^{(\ell+1)}]_b + \epsilon_R)\}$ converge to a point $\{(\mathbf{w}^*, [\boldsymbol{\theta}^*]_b + \epsilon_R)\}$ which is the solution obtained from solving (P2) and (P1.1).

Next, we prove that the converged point $\hat{X}^* \triangleq \{\mathbf{w}^*, \boldsymbol{\theta}^*\}$ is a locally optimal solution of problem P1. For that, we show that the converged point satisfies the Karush-Kuhn-Tucker (KKT) condition of the problem. The KKT condition for problem (P1.1) is satisfied at $\boldsymbol{\theta}^*$. Let $\mathbf{Y}(\boldsymbol{\theta})$ is the objective function of (P3) and $\mathbf{T}(\mathbf{X}) \triangleq [\mathbf{T}_1(\mathbf{X}), \mathbf{T}_2(\mathbf{X}), \dots, \mathbf{T}_I(\mathbf{X})]$ be the set of constraints of problem P3. Then, we can write

$$\begin{aligned} \nabla_{\boldsymbol{\theta}^*} \mathbf{Y}(\mathbf{X}^*) + \mathbf{Z}^T \nabla_{\boldsymbol{\theta}^*} \mathbf{T}(\mathbf{X}^*) &= 0 \\ z_i &\geq 0, t_i \mathbf{T}(\mathbf{X}^*) = 0, \forall i. \end{aligned} \quad (68)$$

where ∇_s is the gradient with respect to s , and $\mathbf{Z} \triangleq [z_1, z_2, \dots, z_I]$ is the optimal Lagrangian variable set. Similarly, the obtained (P2) solution is locally optimal. Hence its KKT is satisfied with respect to $\mathbf{W} = \mathbf{w}_k^*$, which is

$$\begin{aligned} \nabla_{\mathbf{w}^*} \mathbf{Y}(\mathbf{X}^*) + \mathbf{Z}^T \nabla_{\mathbf{w}^*} \mathbf{T}(\mathbf{X}^*) &= 0 \\ z_i &\geq 0, t_i \mathbf{T}(\mathbf{X}^*) = 0, \forall i. \end{aligned} \quad (69)$$

Combining (68) and (69), we get

$$\begin{aligned} \nabla_{\mathbf{X}^*} \mathbf{Y}(\mathbf{X}^*) + \mathbf{Z}^T \nabla_{\mathbf{X}^*} \mathbf{T}(\mathbf{X}^*) &= 0 \\ t_i &\geq 0, t_i \mathbf{T}(\mathbf{X}^*) = 0, \forall i, \end{aligned} \quad (70)$$

which is the KKT condition for (P1). ■

APPENDIX B

PROOF OF LEMMA 1

Let a be a scalar complex variable, and $a^{(\ell)}$ is the fixed point obtained at iteration (ℓ) , then the following inequality holds [19]

$$|a|^2 \geq a^{*,(\ell)} a + a^* a^{(\ell)} - a^{*,(\ell)} a^{(\ell)}, \quad (71)$$

By replacing a with $(\mathbf{u}_k \Phi \mathbf{G}_{\text{AR}}) \mathbf{w}_k$ we obtain (41). Thus, this concludes the proof. ■

APPENDIX C
PROOF OF THEOREM 2, AND 3

Similar to the proof of Theorem 1, it can be shown the sequence $\text{SR}_k(\mathbf{w}^{(\iota+1)}, [\boldsymbol{\theta}_n^{(\iota+1)}]_b)$ is non-decreasing for all k , i.e. $\text{SR}_k(\mathbf{w}^{(\iota+1)}, [\boldsymbol{\theta}_n^{(\iota+1)}]_b) \geq \text{SR}_k(\mathbf{w}^{(\iota)}, [\boldsymbol{\theta}_n^{(\iota)}]_b)$ for all $(\iota) > 0$, and the converged point is a locally optimal solution for problems. ■.

APPENDIX D
INEQUALITIES

Here, we adopt the inequality (48) in [27]. Specifically, for any \mathbf{A} and \mathbf{F} with $\hat{\Lambda}$ and \hat{F} are fixed point, (65) holds.

Next, we adopt Lemma (2) in [24]. Specifically, for any z_i with $i = 1, \dots, l$ and \bar{z}_i is a fixed point, inequality (66) holds. Lastly, the logarithmic function is a concave function and can be written as [24, Eq. 15]

$$-\ln(1 + \Upsilon) \geq -\ln(1 + \bar{\Upsilon}) - \frac{1 + \Upsilon}{1 + \bar{\Upsilon}} + 1. \quad (72)$$

REFERENCES

- [1] T. V. Nguyen, D. N. Nguyen, M. D. Renzo, and R. Zhang, "Leveraging secondary reflections and mitigating interference in multi-IRS/RIS aided wireless networks," *IEEE Transactions on Wireless Communications*, vol. 22, no. 1, pp. 502–517, 2023.
- [2] M. Abughalwa, H. D. Tuan, D. N. Nguyen, H. V. Poor, and L. Hanzo, "Finite-blocklength RIS-aided transmit beamforming," *IEEE Transactions on Vehicular Technology*, vol. 71, no. 11, pp. 12 374–12 379, 2022.
- [3] G. Chen, Q. Wu, C. He, W. Chen, J. Tang, and S. Jin, "Active IRS aided multiple access for energy-constrained IoT systems," *IEEE Transactions on Wireless Communications*, vol. 22, no. 3, pp. 1677–1694, 2023.
- [4] G. Zhou, C. Pan, H. Ren, K. Wang, and Z. Peng, "Secure wireless communication in RIS-aided MISO system with hardware impairments," *IEEE Wireless Communications Letters*, vol. 10, no. 6, pp. 1309–1313, 2021.
- [5] S. Hong, C. Pan, H. Ren, K. Wang, K. K. Chai, and A. Nallanathan, "Robust transmission design for intelligent reflecting surface-aided secure communication systems with imperfect cascaded CSI," *IEEE Transactions on Wireless Communications*, vol. 20, no. 4, pp. 2487–2501, 2020.
- [6] W. Hao, J. Li, G. Sun, M. Zeng, and O. A. Dobre, "Securing reconfigurable intelligent surface-aided cell-free networks," *IEEE Transactions on Information Forensics and Security*, vol. 17, pp. 3720–3733, 2022.
- [7] W. Shi, Q. Wu, F. Xiao, F. Shu, and J. Wang, "Secrecy throughput maximization for IRS-aided MIMO wireless powered communication networks," *IEEE Transactions on Communications*, vol. 70, no. 11, pp. 7520–7535, 2022.
- [8] W. Li, W. Yu, H. Liu, and H. Hou, "Robust secrecy rate maximization for IRS-aided MISO communication systems," in *2023 IEEE 13th International Conference on CYBER Technology in Automation, Control, and Intelligent Systems (CYBER)*, 2023, pp. 604–609.
- [9] L. Dong, H.-M. Wang, and H. Xiao, "Secure cognitive radio communication via intelligent reflecting surface," *IEEE Transactions on Communications*, vol. 69, no. 7, pp. 4678–4690, 2021.
- [10] G. Zhou, C. Pan, H. Ren, K. Wang, and A. Nallanathan, "A framework of robust transmission design for IRS-aided MISO communications with imperfect cascaded channels," *IEEE Transactions on Signal Processing*, vol. 68, pp. 5092–5106, 2020.
- [11] X. Tan, Z. Sun, J. M. Jornet, and D. Pados, "Increasing indoor spectrum sharing capacity using smart reflect-array," in *2016 IEEE International Conference on Communications (ICC)*, 2016, pp. 1–6.
- [12] Q. Wu and R. Zhang, "Beamforming optimization for intelligent reflecting surface with discrete phase shifts," in *ICASSP 2019 - 2019 IEEE International Conference on Acoustics, Speech and Signal Processing (ICASSP 2019)*, 2019, pp. 7830–7833.
- [13] Y. Han, W. Tang, S. Jin, C.-K. Wen, and X. Ma, "Large intelligent surface-assisted wireless communication exploiting statistical CSI," *IEEE Transactions on Vehicular Technology*, vol. 68, no. 8, pp. 8238–8242, 2019.
- [14] M.-A. Badiu and J. P. Coon, "Communication through a large reflecting surface with phase errors," *IEEE Wireless Communications Letters*, vol. 9, no. 2, pp. 184–188, 2020.
- [15] F. Fang, Y. Xu, Q.-V. Pham, and Z. Ding, "Energy-efficient design of IRS-NOMA networks," *IEEE Transactions on Vehicular Technology*, vol. 69, no. 11, pp. 14 088–14 092, 2020.
- [16] S. Boyd, L. El Ghaoui, E. Feron, and V. Balakrishnan, *Linear matrix inequalities in system and control theory*. SIAM, 1994.
- [17] H. Niu, Z. Chu, F. Zhou, and Z. Zhu, "Simultaneous transmission and reflection reconfigurable intelligent surface assisted secrecy MISO networks," *IEEE Communications Letters*, vol. 25, no. 11, pp. 3498–3502, 2021.
- [18] S. Lin, Y. Xu, H. Wang, J. Gu, J. Liu, and G. Ding, "Secure multicast communications via RIS against eavesdropping and jamming with imperfect CSI," *IEEE Transactions on Vehicular Technology*, vol. 72, no. 12, pp. 16 805–16 810, 2023.
- [19] G. Zhou, C. Pan, H. Ren, K. Wang, M. D. Renzo, and A. Nallanathan, "Robust beamforming design for intelligent reflecting surface aided MISO communication systems," *IEEE Wireless Communications Letters*, vol. 9, no. 10, pp. 1658–1662, 2020.
- [20] Q.-U.-A. Nadeem, A. Kammoun, A. Chaaban, M. Debbah, and M.-S. Alouini, "Asymptotic max-min SINR analysis of reconfigurable intelligent surface assisted MISO systems," *IEEE Transactions on Wireless Communications*, vol. 19, no. 12, pp. 7748–7764, 2020.
- [21] C. Pan, H. Ren, M. ElKashlan, A. Nallanathan, and L. Hanzo, "Robust beamforming design for ultra-dense user-centric C-RAN in the face of realistic pilot contamination and limited feedback," *IEEE Transactions on Wireless Communications*, vol. 18, no. 2, pp. 780–795, 2019.
- [22] Z. Zhang, L. Lv, Q. Wu, H. Deng, and J. Chen, "Robust and secure communications in intelligent reflecting surface assisted NOMA networks," *IEEE Communications Letters*, vol. 25, no. 3, pp. 739–743, 2021.
- [23] M. Bloch, J. Barros, M. R. D. Rodrigues, and S. W. McLaughlin, "Wireless information-theoretic security," *IEEE Transactions on Information Theory*, vol. 54, no. 6, pp. 2515–2534, 2008.
- [24] H. Niu, Z. Lin, Z. Chu, Z. Zhu, P. Xiao, H. X. Nguyen, I. Lee, and N. Al-Dhahir, "Joint beamforming design for secure RIS-assisted IoT networks," *IEEE Internet of Things Journal*, vol. 10, no. 2, pp. 1628–1641, 2023.
- [25] M. Grant and S. Boyd, "Cvx: Matlab software for disciplined convex programming, version 2.1," 2014.
- [26] Y. Labit, D. Peaucelle, and D. Henrion, "Sedumi interface 1.02: a tool for solving LMI problems with sedumi," in *Proceedings. IEEE International Symposium on Computer Aided Control System Design*. IEEE, 2002, pp. 272–277.
- [27] H. H. M. Tam, H. D. Tuan, and D. T. Ngo, "Successive convex quadratic programming for quality-of-service management in full-duplex MU-MIMO multicell networks," *IEEE Transactions on Communications*, vol. 64, no. 6, pp. 2340–2353, 2016.
- [28] S. Boyd and L. Vandenberghe, *Convex optimization*. Cambridge university press, 2004.
- [29] Y. Eldar, A. Ben-Tal, and A. Nemirovski, "Robust mean-squared error estimation in the presence of model uncertainties," *IEEE Transactions on Signal Processing*, vol. 53, no. 1, pp. 168–181, 2005.
- [30] W. Wang, W. Ni, H. Tian, Z. Yang, C. Huang, and K.-K. Wong, "Safeguarding NOMA networks via reconfigurable dual-functional surface under imperfect CSI," *IEEE Journal of Selected Topics in Signal Processing*, vol. 16, no. 5, pp. 950–966, 2022.
- [31] Y. Chen, Y. Wang, and L. Jiao, "Robust transmission for reconfigurable intelligent surface aided millimeter wave vehicular communications with statistical CSI," *IEEE Transactions on Wireless Communications*, vol. 21, no. 2, pp. 928–944, 2022.
- [32] H.-M. Wang, J. Bai, and L. Dong, "Intelligent reflecting surfaces assisted secure transmission without eavesdropper's CSI," *IEEE Signal Processing Letters*, vol. 27, pp. 1300–1304, 2020.
- [33] H. Niu, X. Lei, Y. Xiao, M. Xiao, and S. Mumtaz, "On the efficient design of RIS-assisted secure MISO transmission," *IEEE Wireless Communications Letters*, vol. 11, no. 8, pp. 1664–1668, 2022.
- [34] A. D. Wyner, "The wire-tap channel," *The Bell System Technical Journal*, vol. 54, no. 8, pp. 1355–1387, 1975.
- [35] E. Björnson, Ö. Özdogan, and E. G. Larsson, "Intelligent reflecting surface versus decode-and-forward: How large surfaces are needed to beat relaying?" *IEEE Wireless Communications Letters*, vol. 9, no. 2, pp. 244–248, 2020.
- [36] R. K. Jain, D.-M. W. Chiu, W. R. Hawe *et al.*, "A quantitative measure of fairness and discrimination," *Eastern Research Laboratory, Digital Equipment Corporation, Hudson, MA*, vol. 21, 1984.